Classification and construction of higher-order symmetry-protected topological phases of interacting bosons

Alex Rasmussen and Yuan-Ming Lu
Department of Physics, The Ohio State University, Columbus, Ohio 43210, USA

(Received 1 October 2018; revised manuscript received 26 August 2019; accepted 27 November 2019; published 25 February 2020)

Motivated by the recent discovery of higher-order topological insulators, we study their counterparts in strongly interacting bosons: "higher-order symmetry-protected topological (HOSPT) phases." While the usual (first-order) SPT phases in d spatial dimensions support anomalous $(d-1)$-dimensional surface states, HOSPT phases in d dimensions are characterized by topological boundary states of dimension $(d-2)$ or smaller, protected by certain global symmetries and robust against disorders. Based on a dimensional reduction analysis, we show that HOSPT phases can be built from lower-dimensional SPT phases in a way that preserves the associated crystalline symmetries. When the total symmetry is a direct product of global and crystalline symmetry groups, we are able to classify the HOSPT phases using the Künneth formula of group cohomology. Based on a decorated domain-wall picture of the Künneth formula, we show how to systematically construct the HOSPT phases, and demonstrate our construction with many examples in two and three dimensions.

DOI: 10.1103/PhysRevB.101.085137

I. INTRODUCTION

The discovery of topological insulators [1–3] (TIs) unveiled a large class of symmetry-protected topological (SPT) states [4,5], which in d spatial dimensions feature symmetry-protected surface states on $(d-1)$-dimensional open boundaries, such as one-dimensional (1D) helical edge states in two-dimensional (2D) quantum spin Hall insulators [6] and 2D Dirac fermions on the surface of three-dimensional (3D) topological insulators [2]. Recently, a new family of "higher-order" topological insulators has been revealed [7–27], which do not have gapless surface states, but exhibit gapless modes on hinges and corners of the system. Generally, a kth-order TI in d dimensions hosts robust gapless excitations on $(d-k)$-dimensional open boundaries of the system: such as zero-dimensional corner states in second-order 2D TIs and third-order 3D TIs, as well as 1D hinge states in second-order 3D TIs. In this terminology, the usual TIs can be called first-order TIs. These lower-dimensional boundary excitations are robust against any small perturbations such as disorders and crystal distortions, as long as the global symmetry G_0 is protected, analogous to the stability of the TI surface states. It has been shown that the higher-order TIs usually also preserve certain crystalline symmetries in addition to the global symmetry [7–13,18,28]. While most of the efforts so far are focused on higher-order topological phases within band theory of noninteracting fermions, little is known about their strongly interacting counterparts in, e.g., interacting boson systems [29,30]. How to understand the higher-order SPT phases in a generic interacting boson system?

The goal of this work is to address this issue. We provide the classification and explicit construction for "strong" higher-order SPT (HOSPT) phases of interacting bosons with various global (i.e., onsite) symmetry G_0 and crystalline symmetry G_c, whose lower-dimensional boundary excitations are protected only by onsite symmetry G_0 and hence robust against disorders and crystal distortions. To do this, we construct the kth-order SPT phases in d spatial dimensions by stacking $(d+1-k)$-dimensional G_0-SPT phases in a way which preserves crystalline symmetry G_c. This construction generalizes the decorated domain-wall picture set out in Ref. [4] to include the crystal symmetry.

The consistency conditions in a decorated domain-wall construction are phrased in terms of cohomology groups. In particular, for total symmetry $G = G_0 \times G_c$ as a direct product of onsite symmetry G_0 and crystalline symmetry G_c, we show that all $(k+1)$th-order SPT phases in d dimensions are classified within the group cohomology

$$\mathcal{H}^k(G_c^*, \mathcal{H}^{d+1-k}(G_0, U(1))), \tag{1}$$

where G_c^* is isomorphic to crystalline group G_c by regarding each orientation-reversing symmetry operation as an antiunitary operator [31,32]. The above classification also provides a procedure to construct these HOSPT phases from building blocks of $(d-k)$-dimensional SPT phases protected by onsite symmetry G_0 only, as illustrated in many examples.

Expanding Eq. (1) using the Künneth formula will yield several terms. By using our construction, we will see that each of these terms is naturally associated with a particular domain-wall configuration. However, since Eq. (1) is believed to classify bosonic SPT phases [32], we conjecture that our construction yields the correct states and classification groups.

This work is organized as follows. First, in Sec. II we discuss the physical picture behind HOSPT phases based on a dimensional reduction point of view. Then, we show the general classification of HOSPT phases in Sec. III A based on the Künneth formula of group cohomology, and how to the construct the HOSPT phases using the decorated domain-wall picture in Sec. III C. The classification and construction are demonstrated for second-order SPT phases in two (Sec. IV)

and three (Sec. V) dimensions, and third-order SPT phases in three dimensions (Sec. VI). We conclude with a few remarks in Sec. VII.

II. PHYSICAL PICTURE

Before introducing the mathematical classification for higher-order SPT phases, we first discuss an intuitive physical picture which shows how higher-order SPT phases can be built by stacking lower-dimensional SPT phases. Throughout this work, we will focus on the simplest situation where the total symmetry group $G = G_c \times G_0$ is a direct product of crystalline symmetry group G_c and onsite (i.e., global) symmetry group G_0.

By definition, a kth-order SPT phase in d dimensions is characterized by symmetry-protected gapless states on boundaries of $(d-k)$ dimensions. For example, as illustrated in Fig. 2, a second-order SPT phase in $d = 2$ with fourfold rotational symmetry $G_c = C_4$ hosts gapless zero modes at each corner of a square-shaped system, which are protected by onsite symmetry G_0. Based on this example and without loss of generality, below we present two arguments to establish a dimensional reduction picture for the HOSPT phases: while the first argument (Sec. II A) shows why a kth-order SPT phase in d dimensions is related to the usual G_0-SPT phases in $(d+1-k)$ dimensions, the second argument (Sec. II B) explicitly demonstrates how to build such a HOSPT phase from lower-dimensional SPT phases. While the first argument explains why the classification of HOSPT phases is determined by the classification of $(d+1-k)$-dimensional SPT phases, the second argument shows which of the $(d+1-k)$-dimensional SPT phases can consistently lead to a gapped symmetric kth-order SPT phase in d dimensions, to be compatible with the crystalline symmetry G_c.

A. Corner/hinge states as gapless defects on the gapped open surface

We consider a generic HOSPT phase $|\psi\rangle$ of order $k \geqslant 2$ on a d-dimensional open manifold $\mathcal{A}$ (such as the square-shaped system in Fig. 1), which is gapped almost everywhere except for a $(d-k)$-dimensional submanifold on the boundary $\partial\mathcal{A}$ (such as the four corners with $k = d = 2$ in Fig. 1). Since by definition the $(d-1)$-dimensional boundary $\partial\mathcal{A}$ is gapped, this is not a "strong" SPT phase protected by onsite symmetry G_0 only, and hence there exists a finite-depth quantum circuit [4] $\hat{U}$,

$$\hat{U}|\psi\rangle = |T\rangle, \tag{2}$$

which continuously evolves the HOSPT state $|\psi\rangle$ into a trivial product state $|T\rangle$, while preserving onsite symmetry G_0. We label the finite depth of circuit $\hat{U}$ as d_U.

As illustrated in Fig. 1, next we divide the total system $\mathcal{A}$ into two regions: its (simply connected) interior $\mathcal{B}_0$ (both white and gray in Fig. 1), and boundary $\bar{\mathcal{B}}_0 = \mathcal{A} \setminus \mathcal{B}_0$. We can then define a finite-depth (d_U) quantum circuit $U_{\mathcal{B}_0} = P_{\mathcal{B}_0}\hat{U}P_{\mathcal{B}_0}$ by restricting quantum circuit $\hat{U}$ into region $\mathcal{B}_0$, such that

$$\hat{U}_{\mathcal{B}_0}|\psi\rangle = |T_{\mathcal{B}}\rangle \otimes |\psi_{\bar{\mathcal{B}}}\rangle, \tag{3}$$

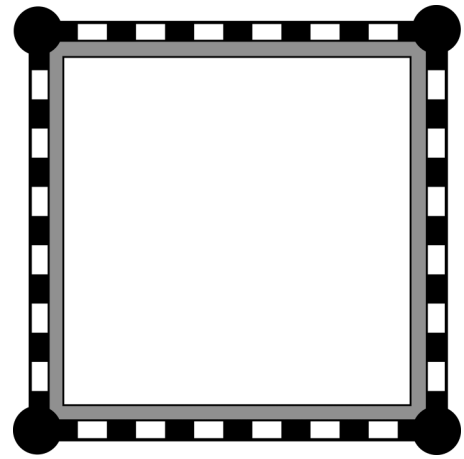

FIG. 1. Disentangling the gapped bulk with gapless corner states. The interior region $\mathcal{B}$ is colored in white, while the "cushion" region $\mathcal{B}_0 \setminus \mathcal{B}$ is colored in gray. Finite-depth quantum circuit $\hat{U}_{\mathcal{B}_0}$ preserving onsite symmetry G_0 will trivialize the interior $\mathcal{B}$ into a product state, while keeping the boundary $\bar{\mathcal{B}}_0 = \mathcal{A} \setminus \mathcal{B}_0$ (including the gapless corner states) untouched.

where $\mathcal{B} \subset \mathcal{B}_0$ is the interior (white in Fig. 1) of $\mathcal{B}_0$, differing from $\mathcal{B}_0$ only by a "cushion" region (gray in Fig. 1) whose width is of the order $\sim d_U$. Here, $|T_{\mathcal{B}}\rangle$ denotes the trivial product state on region $\mathcal{B}$. In other words, finite-depth quantum circuit $U_{\mathcal{B}_0}$ can continuously tune the interior region $\mathcal{B}$ of HOSPT phase into a trivial product state without closing the gap or breaking onsite symmetry G_0, while keeping the boundary states (on $\bar{\mathcal{B}}_0$) untouched. As a result, through finite-depth quantum circuit $\hat{U}_{\mathcal{B}_0}$ which preserves onsite symmetry G_0, the HOSPT ground state is disentangled into a trivial product state $|T_{\mathcal{B}}\rangle$ in the bulk $\mathcal{B}$, and a state $|\psi_{\bar{\mathcal{B}}}\rangle$ on its $(d-1)$-dimensional surface $\bar{\mathcal{B}}$.

Notice that in addition to preserving onsite symmetry G_0, the $(d-1)$-dimensional state $|\psi_{\bar{\mathcal{B}}}\rangle$ is mostly gapped except for hosting gapless modes on its $(d-k)$-dimensional submanifolds. Therefore, the gapless corner/hinge states in a HOSPT can be viewed as gapless $(d-k)$-dimensional defects on a gapped $(d-1)$-dimensional surface state $|\psi_{\bar{\mathcal{B}}}\rangle$ with onsite symmetry G_0. As argued in Refs. [33,34], the classification of such a defect falls in the classification of a $(d+1-k)$-dimensional SPT phase protected by the same onsite symmetry G_0.

These corner or hinge modes have two important properties. First, they are protected by G_0 and possibly also by G_c. As we will see below, there are two types of action of G_c on the boundary modes: either it permutes them or acts onsite. We are mostly interested in the first type, but will enumerate both below. Second, the boundary modes are protected in the thermodynamic limit. Trying to attach a $(k+1)$-dimensional state to trivialize k-dimensional corner or hinge modes cannot be done with a symmetry-respecting finite-depth quantum circuit in the limit of infinite system size.

For example, in a second-order SPT phase in $d = k = 2$, the gapless corner states in, e.g., Fig. 1, can be viewed as gapless zero-dimensional domain walls on the gapped 1D edge. Therefore, they are reduced to the one-dimensional G_0-SPT phases. Similarly for a second-order SPT phase in

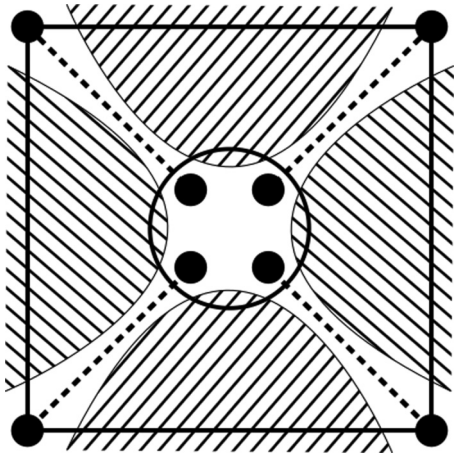

FIG. 2. Dimensional reduction analysis of a second-order SPT phase with $G_c = C_4$ crystalline symmetry, where the black dots represent robust corner zero modes protected by onsite symmetry G_0. Shaded regions are trivialized by the action of a local, finite-depth quantum circuit. Dashed lines represent "effective" one-dimensional (1D) G_0-SPTs, as building blocks for the second-order SPT phase in two dimensions. Note that the four end points of the 1D G_0-SPT phases must fuse to a linear representation in the bulk (circle in the middle), imposing a compatibility condition on the topological index of 1D G_0-SPT phases.

$d = 3$, the gapless hinge states can be viewed as gapless 1D domain walls on a gapped 2D surface, therefore related to two-dimensional G_0-SPT phases. For a third-order SPT phase in $d = k = 3$, the gapless corner states should be viewed as gapless zero-dimensional point defects on the gapped 2D surface with symmetry G_0, hence reduced to one-dimensional G_0-SPT phases.

B. Building HOSPT phases from lower-dimensional SPT phases

In the previous argument, we have shown that the gapless $(d-k)$-dimensional boundary states in a kth-order SPT phase in d dimensions can be reduced to the classification of $(d+1-k)$-dimensional SPT phases preserved only by onsite symmetry G_0. However, not all of the G_0-SPT phases can lead to a gapped HOSPT phase that preserves crystalline symmetry G_c: certain compatibility conditions must be satisfied to ensure a gapped bulk. Here, we provide another argument based on the dimensional reduction approach [35–37], which explicitly builds the kth-order SPT phases in d dimensions out of $(d-k)$-dimensional G_0-SPT phases.

Without loss of generality, we demonstrate this dimensional reduction argument using the second-order 2D SPT phase with $G_c = C_4$ point-group symmetry, as shown in Fig. 2. We first divide the whole open manifold $\mathcal{A}$ into four disconnected shaded regions $\{R_i | 1 \leqslant i \leqslant 4\}$ in Fig. 2 which are related by C_4 symmetry, while both the C_4 inversion center and four gapless corners lie in the rest of the space $\mathcal{A} \setminus (\bigcup_i R_i)$. Following the same construction as used in the previous argument, we can construct a G_0-preserving finite-depth quantum circuit $\hat{U}_{R_1}$ by restricting circuit $\hat{U}$ in region R_1, such that

$$\hat{U}_{R_1}|\psi\rangle = \left|T_{R_1}\right\rangle \otimes \left|\psi_{\bar{R}_1}\right\rangle, \tag{4}$$

where $|T_{R_1}\rangle$ represents the trivial product state on region R_1. By symmetrizing circuit U_{R_1} with respect to C_4 rotations, we can construct a symmetric finite-depth quantum circuit

$$U_R^{\text{sym}} = \prod_{i=0}^{3} (C_4)^i \hat{U}_{R_1} (C_4)^{-i}, \quad R \equiv \bigcup_i R_i, \tag{5}$$

which preserves both onsite symmetry G_0 and crystalline symmetry G_c, such that

$$\hat{U}_R^{\text{sym}}|\psi\rangle = |T_R\rangle \bigotimes |\psi_{\bar{R}}\rangle. \tag{6}$$

In other words, symmetric finite-depth circuit U_R^{sym} trivializes most of the manifold $\mathcal{A}$, except for the four 1D systems connecting the gapless corner to the rotation center. As argued previously, now that each corner state carries a projective representation of onsite symmetry G_0 as the boundary state of a 1D G_0-SPT phase, each 1D system connecting the corner to the C_4 rotation center must be a 1D G_0-SPT phase with a topological index

$$\nu \in \mathcal{H}^2(G_0, U(1)). \tag{7}$$

Note that as a part of the gapped bulk, the C_4 rotation center where the ends of the four 1D G_0-SPT chains must form a linear representation of onsite symmetry G_0, i.e.,

$$4\nu \simeq 0 \in \mathcal{H}^2(G_0, U(1)). \tag{8}$$

This compatibility condition comes from the fusion of a number of edges of 1D SPTs dictated by the crystal symmetry $G_c = C_4$:

$$\phi : \ \mathcal{H}^{d+1-k}(G_0, U(1)) \to \mathcal{H}^{d+1}(G, U(1)). \tag{9}$$

Physically, the fusion map ϕ encodes a notion of compatibility between onsite symmetry G_0 and crystalline symmetry G_c, so that the bulk of the full system is trivial and gapped. Constructing the map ϕ is generally a difficult mathematical problem for an arbitrary symmetry group G with both onsite and crystalline symmetries. In this paper we consider the simplest case, where the symmetry group $G = G_0 \times G_c$ is a direct product of onsite symmetry G_0 and global symmetry G_c. As we will show later, this allows a direct reduction via the Künneth formula, where the compatibility conditions between $(d-k)$-dimensional G_0-SPT phases and crystalline symmetry G_c in d spatial dimensions are captured by group cohomology formula (1).

Finally, we recall that certain SPT phases are beyond the group cohomology classification, such as the 3D time-reversal SPT phase with *efmf* surface topological orders [38,39] classified by cobordism [40,41] and Kitaev's chiral 2D E_8 state [42,43]. We have also considered these beyond-group-cohomology HOSPT phases built from the E_8 state, as highlighted in red in Table II.

III. CLASSIFICATION AND CONSTRUCTION FROM KÜNNETH FORMULA

A. General classification of HOSPT phases

In this work, we will focus on the cases where the total symmetry group G is a direct product of crystalline symmetry

G_c and onsite symmetry G_0:

$$G = G_c \times G_0. \tag{10}$$

In this situation, there is a simple mathematical formula based on group cohomology, which gives the full classification of higher-order SPT phases. It has been shown [31,32] within the group cohomology classification of SPT phases that all G_s symmetry-protected topological phases of interacting bosons in d spatial dimensions are given by

$$\mathcal{H}^{d+1}(G^*, U(1)) = \mathcal{H}^{d+1}(G_c^* \times G_0, U(1)), \tag{11}$$

where G_c^* is isomorphic to G_c, obtained by replacing each orientation-reversing element of crystalline symmetry group G_c by an antiunitary operation of the same rank. According to the Künneth formula for group cohomology [44–46] we have

$$\begin{aligned}
&\mathcal{H}^{d+1}(G_c^* \times G_0, U(1)) = \mathcal{H}^{d+2}(G_c^* \times G_0, \mathbb{Z}) \\
&= \oplus_{k=0}^{d+2} \mathcal{H}^k(G_c^*, \mathcal{H}^{d+2-k}(G_s, \mathbb{Z})) \\
&= \mathcal{H}^{d+1}(G_c^*, U(1)) \oplus \mathcal{H}^{d+1}(G_c^*, \mathcal{H}^1(G_0, \mathbb{Z})) \\
&\quad \oplus_{k=0}^{d} \mathcal{H}^k(G_c^*, \mathcal{H}^{d-k+1}(G_0, U(1))).
\end{aligned} \tag{12}$$

The first term $\mathcal{H}^{d+1}(G_c^*, U(1))$ classifies crystalline SPT phases protected only by crystalline symmetry G_c [32,35]. The second term $\mathcal{H}^{d+1}(G_c^*, \mathcal{H}^1(G_0, \mathbb{Z}))$ vanishes for any finite group [46], as in the case considered here where G_c is a point group or magnetic point group.

Therefore, we shall focus on the last line of the above Künneth formula (12). Each term in

$$\mathcal{H}^k(G_c^*, \mathcal{H}^{d-k+1}(G_0, U(1))), \quad 0 \leqslant k \leqslant d \tag{13}$$

can be interpreted as the classification of $(k+1)$th-order SPT phases in d spatial dimensions, protected by onsite symmetry G_0 and crystalline symmetry G_c. Such a SPT phase is featured by robust gapless states on proper $(d-k-1)$-dimensional open boundaries, which are protected by onsite symmetry G_0 alone. For example, the $k=0$ term in (13)

$$\mathcal{H}^0(G_c^*, \mathcal{H}^{d+1}(G_0, U(1))) = \mathcal{H}^{d+1}(G_0, U(1)) \tag{14}$$

corresponds to the first-order (i.e., the usual "strong") SPT phases protected by onsite symmetry G_0, featured by gapless modes on $(d-1)$-dimensional boundaries.

Second-order SPT phases in $d \geqslant 2$ are all captured by $k=1$ term in (13),

$$\mathcal{H}^1(G_c^*, \mathcal{H}^d(G_0, U(1))), \tag{15}$$

which hosts gapless (or anomalous topological orders when $d \geqslant 4$) excitations on $(d-2)$-dimensional boundaries protected by onsite symmetry G_0.

Similarly, third-order SPT phases in $d \geqslant 3$ are all captured by $k=2$ term in (13),

$$\mathcal{H}^2(G_c^*, \mathcal{H}^{d-1}(G_0, U(1))), \tag{16}$$

which hosts gapless (or anomalous topological orders when $d \geqslant 5$) excitations on $(d-3)$-dimensional boundaries protected by onsite symmetry G_0, such as corner states in $d=3$.

B. "Strong" HOSPT phases versus "weak" crystalline SPT phases

As mentioned previously, we define kth-order SPT phases in d dimensions by the presence of robust $(d-k)$-dimensional topological boundary states, protected by onsite (or global) symmetry G_0 only. These are "strong" SPT phases, whose boundary excitations do not require protection from the crystalline symmetry G_c. In comparison, there are also "weak" crystalline SPT phases, whose topological boundary excitations are protected by crystalline symmetries (in addition to onsite symmetries) [32,47–49]. In fact, in addition to strong HOSPT phases which are the focus of this paper, certain weak crystalline SPT phases are encoded inside the whole Künneth formula (12), such as those colored in green in Table III. Before systematically analyzing and constructing HOSPT phases in detail, we briefly discuss the weak crystalline SPT phases.

First of all, the $k = d+1$ term $\mathcal{H}^{d+1}(G_c^*, U(1))$ in Künneth formula clearly describes weak SPT phases protected only by the crystalline symmetry G_c. Next, we comment on $k=d$ term in (13):

$$\mathcal{H}^d(G_c^*, \mathcal{H}^1(G_0, U(1))). \tag{17}$$

The physics of this term is to assign onsite symmetry charges [linear representation $\mathcal{H}^1(G_0, U(1))$ of onsite symmetry G_0] to defects of the crystalline symmetry G_c. In a simplest example, for the $k=d=1$ case of 1D insulators [$G_0 = U(1)$] with inversion symmetry I ($G_c = Z_2^{\mathcal{I}}$), we have $\mathcal{H}^1(U(1), U(1)) = \mathbb{Z}$ and hence

$$\mathcal{H}^1(G_c^*, \mathcal{H}^1(U(1), U(1))) = \mathcal{H}^1\left(Z_2^{\mathcal{I}}, \mathbb{Z}\right) = \mathbb{Z}_2. \tag{18}$$

The nontrivial element of the above $\mathbb{Z}_2$ classification corresponds to assigning an odd number of $U(1)$ charges to the inversion center, while the trivial element corresponds to having an even number of $U(1)$ charge on the inversion center. There are no gapless boundary excitations for either of the two phases in 1D.

However, in $k = d \geqslant 2$, weak SPT phases with boundary states protected by crystalline symmetry generally can appear in the Künneth formula (12). For example, in $k=d=2$ case with mirror symmetry $G_c = Z_2^{\mathcal{M}}$, $\mathcal{H}^2(Z_2^{\mathcal{M}}, \mathcal{H}^1(G_0, U(1)))$ corresponds to assigning G_0 charges to each domain wall of mirror symmetry $\mathcal{M}$ on the 1D mirror axis of the 2D system. This leads to gapless boundary states if the boundary of the system preserves mirror symmetry. Similarly, in the $d=k=3$ case with n-fold rotational symmetry $G_c = C_n$, $\mathcal{H}^3(C_n, \mathcal{H}^1(G_0, U(1)))$ corresponds to assigning G_0 charges to each domain wall of C_n rotational symmetry on the 1D rotation axis. This leads to weak 3D crystalline SPT phases, hosting gapless (or anomalous) boundary states if the boundary preserves C_n symmetry.

Another example is $k = d-1$ in (13). Take $d=3$, $k=2$ for instance, considering mirror symmetry $G_c = Z_2^{\mathcal{M}}$ again, $\mathcal{H}^2(Z_2^{\mathcal{M}}, \mathcal{H}^2(G_0, U(1)))$ corresponds to assigning 1D G_0-SPT phases classified by $\mathcal{H}^2(G_0, U(1))$ to each mirror domain wall on the 2D mirror plane. This can lead to gapless (or anomalous) boundary states protected by both mirror and onsite G_0 symmetry, if the boundary preserves mirror symmetry $\mathcal{M}$.

As we mentioned before, the boundary states of these weak crystalline SPT phases will generally be destroyed by perturbations that break the crystalline symmetry, such as disorders and crystalline distortions. Meanwhile, their interpretation in the Künneth formula can be quite tricky, as shown in the above examples. Hereafter, we will be focusing on the strong HOSPT phases, whose topological boundary excitations are robust even if crystalline symmetries are broken on the surface.

C. Decorated domain-wall construction

Here, we briefly describe how to explicitly construct the higher-order SPT phases in d spatial dimensions, using G_0-SPT phases in lower dimensions. In particular, the group cohomology formula (13) provides a clear physical meaning for such a construction, similar to the decorated domain-wall construction [50] for the usual ("first-order") SPT phases.

First, we consider second-order SPT phases in d dimensions, classified by first group cohomology

$$\{\nu_1(g_0, g_1) \in \mathcal{H}^d(G_0, U(1)) | g_i \in G_c^*\} \in \mathcal{H}^1(G_c^*, \mathcal{H}^d(G_0, U(1))). \tag{19}$$

These are nothing but linear representations of the symmetry group G_c^*,

$$U_g \equiv \nu_1(1, g) \in \mathcal{H}^d(G_0, U(1)), \quad g \in G_c^* \tag{20}$$

satisfying the 1-cocycle condition

$$U_g U_h^{s(g)} = U_{gh}, \quad s(g) = \pm 1 \text{ for } g = \text{unitary/antiunitary}. \tag{21}$$

U_g valued in $\mathcal{H}^d(G_0, U(1))$ physically represents a domain wall labeled by symmetry element g, decorated by $(d-1)$-dimensional G_0-SPT phases labeled by elements in $\mathcal{H}^d(G_0, U(1))$. The above 1-cocycle condition can be viewed as a compatibility condition between the addition rules of $(d-1)$-dimensional G_0-SPT phases and the addition rules ($gh = gh$) of domain walls, in order to ensure a gapped bulk spectrum. To understand this, we see that a domain wall of the G_c^* symmetry is labeled by a group element $g_1 \in G_c^*$. The $(d-1)$-dimensional SPT phase associated with this domain wall is labeled by an element $m_1 \in \mathcal{H}^d(G_0, U(1))$. The fusion of two domain walls $g_1 g_2$ combines these $(d-1)$-dimensional G_0-SPT's into $m_1 + m_2$. However, the fusion must respect the group structure of $\mathcal{H}^d(G_0, U(1))$, and this consistency condition is exactly captured by Eq. (13). Therefore, each element of $\mathcal{H}^1(G_c^*, \mathcal{H}^d(G_0, U(1)))$ describes a way to assign $(d-1)$-dimensional G_0-SPT phases on the domain walls of crystalline symmetry G_c, which is compatible with a gapped bulk.

Next, we consider second-order SPT phases in d dimensions, classified by second group cohomology

$$\{\nu_2(g_0, g_1, g_2) \in \mathcal{H}^{d-1}(G_0, U(1)) | g_i \in G_c^*\} \in \mathcal{H}^2(G_c^*, \mathcal{H}^{d-1}(G_0, U(1))). \tag{22}$$

They are nothing but projective representation of symmetry group G_c^*,

$$U_g U_h^{s(g)} = \omega(g, h) U_{gh}, \quad g, h \in G_c^*; \tag{23}$$

$$\omega(g, h) \equiv \nu_2(1, g, gh) \in \mathcal{H}^{d-1}(G_0, U(1)), \tag{24}$$

satisfying the 2-cocycle (or associativity) condition

$$\omega(g, h)\omega(gh, k) = \omega(g, hk)\omega^{s(g)}(h, k), \quad g, h, k \in G_c^*. \tag{25}$$

Since U_g represents the $(d-1)$-dimensional domain wall labeled by element g of crystalline symmetry G_c^*, $\omega(g, h)$ naturally represents the $(d-2)$-dimensional manifold where three domain walls U_g, U_h, and $U_{(gh)^{-1}}$ intersect. The fact that $\omega(g, h)$ takes values in $\mathcal{H}^{d-1}(G_0, U(1))$ physically means that these domain-wall intersections are decorated by $(d-2)$-dimensional G_0-SPT phases, which are classified by group cohomology $\mathcal{H}^{d-1}(G_0, U(1))$.

As a simplest example, we consider the n-fold rotational symmetry $G_c = C_n$. Each of the n domain walls of the C_n symmetry can be decorated by the same $(d-1)$-dimensional G_0-SPT phase, such that n copies of these G_0-SPT phases intersect at the C_n rotational axis. For the system to be gapped on the rotational axis, these n copies of G_0-SPT phases together must fuse to a trivial phase with no gapless boundary states. This exactly corresponds to second-order SPT phases classified by $\mathcal{H}^1(C_n^* \simeq Z_n, \mathcal{H}^d(G_0, U(1)))$. Meanwhile, at the intersection of n domain walls of C_n symmetry, the rotational axis itself can also be decorated by a $(d-2)$-dimensional G_0-SPT phase, which corresponds to the third-order SPT phases classified by $\mathcal{H}^2(C_n^* \simeq Z_n, \mathcal{H}^{d-1}(G_0, U(1)))$.

Another example is the mirror reflection symmetry $G_c = Z_2^{\mathcal{M}}$, where the orientation-reversing mirror symmetry $\mathcal{M}$ should be regarded as an antiunitary symmetry when computing the group cohomology. For $k = d = 2$, the second-order SPT phases in classified by $\mathcal{H}^1(Z_2^{\mathcal{M}}, \mathcal{H}^2(G_0, U(1)))$ can be understood as assigning a 1D G_0-SPT phase on each mirror plane.

Below we will classify second-order SPT phases in $d = 2, 3$ (Tables I and II) and third-order SPT phases in $d = 3$ (Table III), for various choices of onsite symmetry G_0 and crystalline (and magnetic crystalline) symmetry G_c. We will also explicitly construct these higher-order SPT phases using the decorated domain-wall picture as described above in Secs. IV–VI.

IV. SECOND-ORDER SPT PHASES IN TWO DIMENSIONS

As shown in (15), the second-order SPT phases in d spatial dimensions are classified by $\mathcal{H}^{k=1}(G_c^*, \mathcal{H}^d(G_0, U(1)))$, i.e., the linear representation of group G_c^* whose coefficients take value in the $(d-1)$-dimensional SPT classification $\mathcal{H}^d(G_0, U(1))$. For $d = 2$ case, the building blocks of second-order SPT phases in two dimensions are 1D SPT phases protected by onsite symmetry G_0. Below, we provide a full classification for second-order SPT phases in $d = 2$ with all possible 2D point-group and magnetic point-group symmetries, and describe how to use 1D SPT phases to construct these second-order 2D SPT phases.

A. Classification

To compute $\mathcal{H}^1(G_c^*, \mathcal{H}^d(G_0, U(1)))$, first we need to obtain the group G_c^* from crystalline symmetry G_c. As mentioned earlier, G_c^* is isomorphic to G_c, obtained by replacing each

TABLE I. Second-order bosonic SPT phases ($k = 1$) in $d = 2$ spatial dimensions, protected by symmetry group $G_s = G_c \times G_0$ where G_c and G_0 represent the crystalline and onsite symmetry group, respectively. The general classification is given by linear representation $\mathcal{H}^1(G_c^*, \mathcal{H}^2(G_0, U(1)))$ as shown in (15) with $d = 2$. Through a dimensional reduction procedure they are all constructed from G_0-SPT phases in $d = 1$ dimension, classified by $\mathcal{H}^2(G_0, U(1))$ in the last line (blue).

$k = 1, d = 2$	Onsite symmetry G_0				
Crystalline symmetry G_c	$Z_2^{\mathcal{T}}$	$SO(3)$ or $U(1) \rtimes Z_2$	$SO(3) \times Z_2^{\mathcal{T}}$ or $U(1) \times Z_2^{\mathcal{T}}$	$Z_a \times Z_b$	$Z_a \times Z_2^{\mathcal{T}}$
C_n	$\mathbb{Z}_{(n,2)}$	$\mathbb{Z}_{(n,2)}$	$\mathbb{Z}_{(n,2)}$	$\mathbb{Z}_{(n,a,b)}$	$\mathbb{Z}_{(n,2)} \times \mathbb{Z}_{(n,a,2)}$
$C_{n,\mathrm{v}} = C_n \rtimes Z_2^{\mathcal{M}_\mathrm{v}}$	$\mathbb{Z}_{(n,2)} \times \mathbb{Z}_2$	$\mathbb{Z}_{(n,2)} \times \mathbb{Z}_2$	$\mathbb{Z}^2_{(n,2)} \times \mathbb{Z}_2^2$	$\mathbb{Z}_{(n,a,b)} \times \mathbb{Z}_{(2,a,b)}$	$\mathbb{Z}_{(n,2)} \times \mathbb{Z}_{(n,a,2)} \times \mathbb{Z}_2 \times \mathbb{Z}_{(a,2)}$
$C_{2n}^{\mathcal{T}} \equiv \{(c_{2n} \cdot \mathcal{T})^m \vert 0 \leqslant m < 2n\}$	$\mathbb{Z}_2$	$\mathbb{Z}_2$	$\mathbb{Z}_2^2$	$\mathbb{Z}_{(2,a,b)}$	$\mathbb{Z}_2 \times \mathbb{Z}_{(a,2)}$
$C_{2n}^{\mathcal{T}} \rtimes Z_2^{\mathcal{M}_\mathrm{v}}$	$\mathbb{Z}_2^2$	$\mathbb{Z}_2^2$	$\mathbb{Z}_2^4$	$\mathbb{Z}^2_{(2,a,b)}$	$\mathbb{Z}_2^2 \times \mathbb{Z}^2_{(a,2)}$
$C_n \rtimes Z_2^{\mathcal{M}_\mathrm{v} \cdot \mathcal{T}}$	$\mathbb{Z}_{(n,2)} \times \mathbb{Z}_2$	$\mathbb{Z}_{(n,2)} \times \mathbb{Z}_2$	$\mathbb{Z}^2_{(n,2)} \times \mathbb{Z}_2^2$	$\mathbb{Z}_{(2,n,a,b)} \times \mathbb{Z}_{(2,a,b)}$	$\mathbb{Z}_{(n,2)} \times \mathbb{Z}_{(n,a,2)} \times \mathbb{Z}_2 \times \mathbb{Z}_{(a,2)}$
$d = 1$ G_0-SPTs: $\mathcal{H}^2(G_0, U(1))$	$\mathbb{Z}_2$	$\mathbb{Z}_2$	$\mathbb{Z}_2^2$	$\mathbb{Z}_{(a,b)}$	$\mathbb{Z}_2 \times \mathbb{Z}_{(a,2)}$

orientation-reversing element g of G_c by an antiunitary operation g^* of the same rank. For example, we have

$$G_c = C_n \Longrightarrow G_c^* \simeq Z_n; \tag{26}$$

$$G_c = C_n \rtimes Z_2^{\mathcal{M}_\mathrm{v}} \Longrightarrow G_c^* \simeq Z_n \rtimes Z_2^{\mathcal{T}}; \tag{27}$$

$$G_c = C_{2n}^{\mathcal{T}} \text{ or } S_{2n} \Longrightarrow G_c^* \simeq, \tag{28}$$

where we use $Z_{2n}^{\mathcal{T}}$ to denote a group generated by an antiunitary operator $\mathcal{T}$ of ranking $2n$.

After obtaining G_c^*, the next step is to compute $\mathcal{H}^d(G_0, U(1))$, the coefficient of the desired linear representation $\mathcal{H}^1$. For $d = 2$ case, $\mathcal{H}^2(G_0, U(1))$ corresponds to the classification of 1D SPT phases [51–54] protected by onsite symmetry G_0: it always forms a finite Abelian group, as summarized in the last line of Table I.

Generally, the classification of SPT phases with onsite symmetry G_0 always forms a discrete Abelian group, which holds for the group cohomology classification $\mathcal{H}^d(G_0, U(1))$ and beyond. One important relation for group cohomology is

$$\mathcal{H}^k(G, A \times B) = \mathcal{H}^k(G, A) \times \mathcal{H}^k(G, B). \tag{29}$$

Therefore, to compute $\mathcal{H}^1(G_c^*, \mathcal{H}^d(G_0, U(1)))$ in (15), we only need to know $\mathcal{H}^1(G, \mathbb{Z})$, and $\mathcal{H}^1(G, \mathbb{Z}_a)$ for any finite integer $a \in \mathbb{Z}$. Since $\mathcal{H}^2(G_0, U(1))$ is always a finite Abelian group, making use of relation (29), we can compute $\mathcal{H}^1(G_c^*, \mathcal{H}^2(G_0, U(1)))$ purely based on knowledge of $\mathcal{H}^1(G, \mathbb{Z}_a)$ for any finite integer a. Below, we list $\mathcal{H}^1(G_c^*, \mathbb{Z}_a)$ for all $d = 2$ point groups and magnetic point groups G_c:

$$(C_n)^* \simeq Z_n, \quad \left(S_{2n}^{\mathcal{T}}\right)^* \simeq Z_{2n}, \quad \mathcal{H}^1(Z_n, \mathbb{Z}_a) = \mathbb{Z}_{(n,a)}; \tag{30}$$

$$(C_{n,\mathrm{v}})^* \simeq \left(C_n \rtimes Z_2^{\mathcal{M}_\mathrm{v}\mathcal{M}_\mathrm{h}\mathcal{T}}\right)^* \simeq Z_n \rtimes Z_2^{\mathcal{T}},$$
$$\mathcal{H}^1\left(Z_n \rtimes Z_2^{\mathcal{T}}, \mathbb{Z}_a\right) = \mathbb{Z}_{(n,a)} \times \mathbb{Z}_{(2,a)}; \tag{31}$$

$$\left(C_{2n}^{\mathcal{T}}\right)^* \simeq (S_{2n})^* \simeq Z_{2n}^{\mathcal{T}}; \quad \mathcal{H}^1\left(Z_{2n}^{\mathcal{T}}, \mathbb{Z}_a\right) = \mathbb{Z}_{(2,a)}; \tag{32}$$

TABLE II. Second-order bosonic SPT phases ($k = 1$) in $d = 3$ spatial dimensions, protected by symmetry group $G_s = G_c \times G_0$ where G_c and G_0 represent the crystalline and onsite symmetry group, respectively. The general classification is given by linear representation $\mathcal{H}^1(G_c^*, \mathcal{H}^3(G_0, U(1)))$ as shown in (15) with $d = 3$, except for the "beyond-cohomology" states colored by red. Through a dimensional reduction procedure, they can all be built from G_0-SPT phases in $d = 2$ dimension, classified by $\mathcal{H}^3(G_0, U(1))$ in the last line. Red-colored "beyond-cohomology" states are built from the chiral bosonic E_8 state [42,43].

$k = 1, d = 3$	Onsite symmetry G_0				
Crystalline symmetry G_c	$U(1)$ or $SO(3)$	$U(1) \rtimes Z_2$	$SO(3) \times Z_2^{\mathcal{T}}$	Z_a	$Z_a \times Z_2^{\mathcal{T}}$
C_n	$\mathbb{Z}_1$	$\mathbb{Z}_{(n,2)}$	$\mathbb{Z}_{(n,2)}$	$\mathbb{Z}_{(n,a)}$	$\mathbb{Z}^2_{(n,a,2)}$
$C_{n,\mathrm{v}}$ or $C_n \rtimes Z_2^{\mathcal{M}_\mathrm{v}\mathcal{M}_\mathrm{h}\mathcal{T}}$	$\mathbb{Z}_2 \times \mathbb{Z}_2$	$\mathbb{Z}_2^2 \times \mathbb{Z}_{(n,2)} \times \mathbb{Z}_2$	$\mathbb{Z}_{(n,2)} \times \mathbb{Z}_2$	$\mathbb{Z}_{(n,a)} \times \mathbb{Z}_{(2,a)} \times \mathbb{Z}_2$	$\mathbb{Z}^2_{(n,a,2)} \times \mathbb{Z}^2_{(a,2)}$
$C_{n,\mathrm{h}} \equiv C_n \times Z_2^{\mathcal{M}_\mathrm{h}}$	$\mathbb{Z}_2 \times \mathbb{Z}_2$	$\mathbb{Z}_2^2 \times \mathbb{Z}_{(n,2)} \times \mathbb{Z}_2$	$\mathbb{Z}_{(n,2)} \times \mathbb{Z}_2$	$\mathbb{Z}_{(n,a,2)} \times \mathbb{Z}_{(2,a)} \times \mathbb{Z}_2$	$\mathbb{Z}^2_{(n,a,2)} \times \mathbb{Z}^2_{(a,2)}$
$D_n \equiv C_n \rtimes Z_2^{\mathcal{M}_\mathrm{h} \cdot \mathcal{M}_\mathrm{v}}$ or $C_n \rtimes Z_2^{\mathcal{M}_\mathrm{v} \cdot \mathcal{T}}$	$\mathbb{Z}_1$	$\mathbb{Z}_{(n,2)} \times \mathbb{Z}_2$	$\mathbb{Z}_{(n,2)} \times \mathbb{Z}_2$	$\mathbb{Z}_{(n,a,2)} \times \mathbb{Z}_{(2,a)}$	$\mathbb{Z}^2_{(n,a,2)} \times \mathbb{Z}^2_{(a,2)}$
$D_{n,\mathrm{h}} \equiv C_{n,\mathrm{v}} \times Z_2^{\mathcal{M}_\mathrm{h}}$	$\mathbb{Z}_2 \times \mathbb{Z}_2$	$\mathbb{Z}_2^3 \times \mathbb{Z}_{(n,2)} \times \mathbb{Z}_2$	$\mathbb{Z}_{(n,2)} \times \mathbb{Z}_2^2$	$\mathbb{Z}_{(n,a,2)} \times \mathbb{Z}^2_{(2,a)} \times \mathbb{Z}_2$	$\mathbb{Z}^2_{(n,a,2)} \times \mathbb{Z}^4_{(a,2)}$
$C_{2n}^{\mathcal{T}}$ or $S_{2n} \equiv \{(c_{2n} \cdot \mathcal{M}_\mathrm{h})^m \vert 0 \leqslant m < 2n\}$	$\mathbb{Z}_2 \times \mathbb{Z}_2$	$\mathbb{Z}_2^2 \times \mathbb{Z}_2$	$\mathbb{Z}_2$	$\mathbb{Z}_{(2,a)} \times \mathbb{Z}_2$	$\mathbb{Z}^2_{(2,a)}$
$D_{n,\mathrm{d}} \equiv S_{2n} \rtimes Z_2^{\mathcal{M}_\mathrm{v}}$ or $C_{2n}^{\mathcal{T}} \rtimes Z_2^{\mathcal{M}_\mathrm{v}}$	$\mathbb{Z}_2 \times \mathbb{Z}_2$	$\mathbb{Z}_2^3 \times \mathbb{Z}_2$	$\mathbb{Z}_2^2$	$\mathbb{Z}^2_{(2,a)} \times \mathbb{Z}_2$	$\mathbb{Z}^4_{(2,a)}$
$S_{2n}^{\mathcal{T}} \equiv \{(c_{2n} \cdot \mathcal{M}_\mathrm{h} \cdot \mathcal{T})^m \vert 0 \leqslant m < 2n\}$	$\mathbb{Z}_1$	$\mathbb{Z}_2$	$\mathbb{Z}_2$	$\mathbb{Z}_{(2n,a)}$	$\mathbb{Z}^2_{(a,2)}$
$d = 2$ G_0-SPTs: $\mathcal{H}^3(G_0, U(1))$ plus E_8 state	$\mathbb{Z} \times \mathbb{Z}$	$\mathbb{Z} \times \mathbb{Z}_2 \times \mathbb{Z}$	$\mathbb{Z}_2$	$\mathbb{Z}_a \times \mathbb{Z}$	$\mathbb{Z}^2_{(a,2)}$

TABLE III. Third-order bosonic SPT phases ($k = 1$) in $d = 2$ spatial dimensions, protected by symmetry group $G_s = G_c \times G_0$ where G_c and G_0 represent the crystalline and onsite symmetry group, respectively. The general classification is given by projective representation $\mathcal{H}^2(G_c^*, \mathcal{H}^2(G_0, U(1)))$ as shown in (16) with $d = 3$. Through a dimensional reduction procedure they are all constructed from G_0-SPT phases in $d = 1$ dimensions, classified by $\mathcal{H}^2(G_0, U(1))$ in the last line (blue). To be contrasted with the strong third-order SPT phases in black, the weak crystalline SPT phases included in $\mathcal{H}^2(G_c^*, \mathcal{H}^2(G_0, U(1)))$ are colored in green.

$k = 2, d = 3$	Onsite symmetry G_0			
Crystalline symmetry G_c	$Z_2^{\mathcal{T}}$, $SO(3)$ or $U(1) \rtimes Z_2$	$SO(3) \times Z_2^{\mathcal{T}}$ or $U(1) \times Z_2^{\mathcal{T}}$	$Z_a \times Z_b$	$Z_a \times Z_2^{\mathcal{T}}$
C_n	$\mathbb{Z}_{(2,n)}$	$\mathbb{Z}^2_{(2,n)}$	$\mathbb{Z}_{(n,a,b)}$	$\mathbb{Z}_{(2,n)} \times \mathbb{Z}_{(a,2,n)}$
$C_{n,\mathrm{v}}$	$\mathbb{Z}_{(n,2)} \times \mathbb{Z}_{(n,2)} \times \mathbb{Z}_2$	$\mathbb{Z}^2_{(n,2)} \times \mathbb{Z}^2_{(n,2)} \times \mathbb{Z}^2_2$	$\mathbb{Z}_{(n,a,b)} \times \mathbb{Z}_{(n,a,b,2)} \times \mathbb{Z}_{(2,a,b)}$	$\mathbb{Z}_{(n,2)} \times \mathbb{Z}_{(n,a,2)} \times \mathbb{Z}_{(n,a,2)} \times \mathbb{Z}_{(a,2)} \times \mathbb{Z}_{(n,2)} \times \mathbb{Z}_2$
$C_{n,\mathrm{h}}$	$\mathbb{Z}_{(n,2)} \times \mathbb{Z}_2 \times \mathbb{Z}_2$	$\mathbb{Z}^2_{(n,2)} \times \mathbb{Z}^2_2 \times \mathbb{Z}^2_2$	$\mathbb{Z}_{(n,a,b,2)} \times \mathbb{Z}_{(a,b,2)} \times \mathbb{Z}_{(a,b,2)}$	$\mathbb{Z}_{(n,2)} \times \mathbb{Z}_2 \times \mathbb{Z}_{(n,a,2)} \times \mathbb{Z}_{(a,2)} \times \mathbb{Z}_2 \times \mathbb{Z}_{(a,2)}$
D_n	$\mathbb{Z}_{(n,2)} \times \mathbb{Z}^2_2$	$\mathbb{Z}^2_{(n,2)} \times \mathbb{Z}^4_2$	$\mathbb{Z}_{(n,a,b,2)} \times \mathbb{Z}^2_{(2,a,b)}$	$\mathbb{Z}_{(n,2)} \times \mathbb{Z}^2_2 \times \mathbb{Z}_{(n,a,2)} \times \mathbb{Z}^2_{(a,2)}$
$C_n \rtimes Z_2^{\mathcal{M}_\mathrm{v}\cdot\mathcal{T}}$	$\mathbb{Z}_{(n,2)} \times \mathbb{Z}^2_2$	$\mathbb{Z}^2_{(n,2)} \times \mathbb{Z}^4_2$	$\mathbb{Z}_{(n,a,b,2)} \times \mathbb{Z}^2_{(a,b,2)}$	$\mathbb{Z}_{(n,2)} \times \mathbb{Z}_{(n,a,2)} \times \mathbb{Z}^2_2 \times \mathbb{Z}^2_{(a,2)}$
$D_{n,\mathrm{h}}$	$\mathbb{Z}^2_{(n,2)} \times \mathbb{Z}_2 \times \mathbb{Z}^3_2$	$\mathbb{Z}^4_{(n,2)} \times \mathbb{Z}^2_2 \times \mathbb{Z}^6_2$	$\mathbb{Z}^2_{(n,a,b,2)} \times \mathbb{Z}_{(a,b,2)} \times \mathbb{Z}^3_{(a,b,2)}$	$\mathbb{Z}^2_{(n,2)} \times \mathbb{Z}_2 \times \mathbb{Z}^2_{(n,a,2)} \times \mathbb{Z}_{(a,2)} \times \mathbb{Z}^3_2 \times \mathbb{Z}^3_{(a,2)}$
$C_{2n}^{\mathcal{T}}$ or S_{2n}	$\mathbb{Z}_2$	$\mathbb{Z}^2_2$	$\mathbb{Z}_{(2,a,b)}$	$\mathbb{Z}_2 \times \mathbb{Z}_{(a,2)}$
$C_{2n}^{\mathcal{T}} \rtimes Z_2^{\mathcal{M}_\mathrm{v}}$	$\mathbb{Z}_2 \times \mathbb{Z}^2_2$	$\mathbb{Z}^2_2 \times \mathbb{Z}^4_2$	$\mathbb{Z}_{(a,b,2)} \times \mathbb{Z}^2_{(a,b,2)}$	$\mathbb{Z}_2 \times \mathbb{Z}_{(a,2)} \times \mathbb{Z}^2_2 \times \mathbb{Z}^2_{(a,2)}$
$D_{n,\mathrm{d}}$	$\mathbb{Z}^2_2 \times \mathbb{Z}_2$	$\mathbb{Z}^4_2 \times \mathbb{Z}^2_2$	$\mathbb{Z}^2_{(a,b,2)} \times \mathbb{Z}_{(a,b,2)}$	$\mathbb{Z}^2_2 \times \mathbb{Z}^2_{(a,2)} \times \mathbb{Z}_2 \times \mathbb{Z}_{(a,2)}$
$S_{2n}^{\mathcal{T}}$	$\mathbb{Z}_2$	$\mathbb{Z}^2_2$	$\mathbb{Z}_{(2n,a,b)}$	$\mathbb{Z}_2 \times \mathbb{Z}_{(a,2)}$
$T \simeq A_4$	$\mathbb{Z}_2$	$\mathbb{Z}^2_2$	$\mathbb{Z}_{(3,a,b)} \times \mathbb{Z}_{(2,a,b)}$	$\mathbb{Z}_2 \times \mathbb{Z}_{(a,2)}$
$T_h = T \times Z_2^{\mathcal{I}}$	$\mathbb{Z}^2_2 \times \mathbb{Z}_2$	$\mathbb{Z}^4_2 \times \mathbb{Z}^2_2$	$\mathbb{Z}^2_{(2,a,b)} \times \mathbb{Z}^2_{2,a,b}$	$\mathbb{Z}^2_2 \times \mathbb{Z}^2_{(2,a)} \times \mathbb{Z}_2 \times \mathbb{Z}_{(2,a)}$
$\mathcal{H}^2(G_0, U(1))$	$\mathbb{Z}_2$	$\mathbb{Z}^2_2$	$\mathbb{Z}_{(a,b)}$	$\mathbb{Z}_2 \times \mathbb{Z}_{(a,2)}$

$$(D_{n,\mathrm{d}})^* \simeq \left(C_{2n}^{\mathcal{T}} \rtimes Z_2^{\mathcal{M}_\mathrm{v}}\right)^* \simeq Z_{2n}^{\mathcal{T}} \rtimes Z_2,$$
$$\mathcal{H}^1\left(Z_{2n}^{\mathcal{T}} \rtimes Z_2, \mathbb{Z}_a\right) = \mathbb{Z}^2_{(2,a)}; \tag{33}$$

$$(D_n)^* \simeq \left(C_n \rtimes Z_2^{\mathcal{M}_\mathrm{v}\mathcal{T}}\right)^* \simeq Z_n \rtimes Z_2,$$
$$\mathcal{H}^1(Z_n \rtimes Z_2, \mathbb{Z}_a) = \mathbb{Z}_{(n,a,2)} \times \mathbb{Z}_{(a,2)}; \tag{34}$$

$$(C_{n,\mathrm{h}})^* \simeq \left(C_n \times Z_2^{\mathcal{I}}\right)^* \simeq Z_n \times Z_2^{\mathcal{T}},$$
$$\mathcal{H}^1\left(Z_n \times Z_2^{\mathcal{T}}, \mathbb{Z}_a\right) = \mathbb{Z}_{(n,a,2)} \times \mathbb{Z}_{(2,a)}; \tag{35}$$

$$(D_{n,\mathrm{h}})^* \simeq (Z_n \rtimes Z_2) \times Z_2^{\mathcal{T}},$$
$$\mathcal{H}^1\left((Z_n \rtimes Z_2) \times Z_2^{\mathcal{T}}, \mathbb{Z}_a\right) = \mathbb{Z}_{(n,a,2)} \times \mathbb{Z}^2_{(2,a)}. \tag{36}$$

Using relation (29) and the above results (30)–(36), we acquire the classification of all second-order SPT phases in $d = 2$, as summarized in Table I.

B. Examples

1. $G_c = C_n$

The simplest examples of second-order SPT phases are protected by n-fold rotational symmetry $G_c = C_n$, classified by

$$\mathcal{H}^1(Z_n, \mathcal{H}^2(G_0, U(1))). \tag{37}$$

They can all be built from 1D SPT phases protected by onsite symmetry G_0, where the 1D G_0-SPT phases are aligned in a C_n-symmetric manner as shown in Fig. 3 for $G_c = C_3$ case. Since the end points of n copies of 1D G_0-SPT phases intersect at the center of the system (see Fig. 3), they must form a linear representation of onsite symmetry G_0 to ensure a gapped symmetric bulk. This provides a compatibility condition for the 1D G_0-SPT phases, manifested in the group cohomology formula

$$\mathcal{H}^1(Z_n, \mathbb{Z}_a) = \mathbb{Z}_{(n,a)}, \tag{38}$$

where (n, a) is the greatest common divisor of integers n and a.

Formula (38) can be understood as follows. The group cohomology $\mathcal{H}^1(Z_n, \mathbb{Z}_a)$ stands for linear representation $\{U_g | g \in Z_n\}$ of Z_n group with coefficients in $\mathbb{Z}_a$-valued phase factors

$$\mathbb{Z}_a = \left\{u_j \equiv e^{2\pi \mathrm{i} \frac{j}{a}} \middle| 0 \leqslant \nu < a,\ j \in \mathbb{Z}\right\}. \tag{39}$$

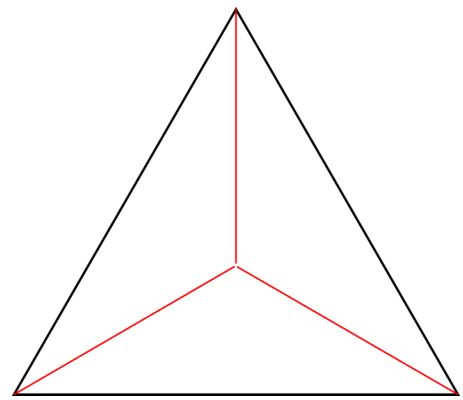

FIG. 3. Second-order SPT phases with $G_c = C_3$ point-group symmetry, where each of the three C_3 domain walls is decorated by the same 1D G_0-SPT phase meeting at the rotation center. The projective representations at the end of each 1D G_0-SPT phase must form a linear representation to ensure a gapped bulk, as manifested in group cohomology formula (15).

Denoting the generator of Z_n group as R with $R^n = 1$, we have

$$U_R|\nu\rangle = u_\nu|\nu\rangle \Longrightarrow U_{1=R^n} = (U_R)^n = u_{n\nu} = 1 \tag{40}$$

and as a result

$$n\nu = 0 \mod a \Longrightarrow \nu = m\frac{a}{(n,a)}, \quad 0 \leqslant m < (n,a) \tag{41}$$

where (n, a) denotes the greatest common divisor of integers a and n. Physically, this means the topological index $\nu \in \mathbb{Z}_a$ of the 1D G_0-SPT phase decorated on each C_n domain wall must be a multiple of $\frac{a}{(n,a)}$, to ensure the bulk to be gapped at the rotation axis where the n domain walls intersect. Hence, there are (n, a) distinct second-order SPT phases with C_n symmetry, characterized by the 1D G_0-SPT phase with $\nu = 0, \frac{a}{(n,a)}, 2\frac{a}{(n,a)}, \ldots$ on each domain wall. This corresponds to the $\mathbb{Z}_{(n,a)}$ classification in formula (38).

One immediate physical consequence is the presence of zero-energy corner modes located on each corner of the C_n-symmetric finite system shown in Fig. 3. Each corner mode is nothing but the boundary states of 1D G_0-SPT phases with $\nu = 0 \mod \frac{a}{(n,a)}$, which carries a projective representation of onsite symmetry G_0. Notice that with only C_n symmetry, the 1D G_0-SPT phases can together be rotated around the C_n center by an arbitrary angle, and therefore the zero-energy corner states will only appear in certain (but not all) finite systems.

2. $G_c = C_{n,v} \equiv C_n \rtimes Z_2^{\mathcal{M}_v}$ or $C_n \rtimes Z_2^{\mathcal{M}_v\mathcal{M}_h\mathcal{T}}$

Consider point group $G_c = C_{n,\mathrm{v}}$, generated by n-fold rotation R with $R^n = 1$ along $\hat{z}$ axis, and mirror reflection $\mathcal{M}_\mathrm{v}$ whose mirror plane is parallel to the $\hat{z}$ axis. As described earlier, the associated second-order SPT phases are classified by the linear representation (first group cohomology) of $(C_{n,\mathrm{v}})^* \simeq Z_n \rtimes Z_2^{\mathcal{T}}$, with coefficients in 1D G_0-SPT phases classified by $\mathcal{H}^2(G_0, U(1))$. The decorated-domain-wall construction of these second-order SPT phases with $C_{n,\mathrm{v}}$ symmetry can be implied from the following formula:

$$\mathcal{H}^1\left(Z_n \rtimes Z_2^{\mathcal{T}}, \mathbb{Z}_a\right) = \mathbb{Z}_{(n,a)} \times \mathbb{Z}_{(2,a)}. \tag{42}$$

The first factor $\mathbb{Z}_{(n,a)}$ labels the 1D G_0-SPT phases assigned on each C_n domain walls and intersected at the C_n rotation center, illustrated by the red lines in Fig. 4. On the other hand, the second factor $\mathbb{Z}_{(2,a)}$ labels the 1D G_0-SPT phases placed on each of the n mirror planes, illustrated by the green lines in Fig. 4. The linear representation $\{U_R, U_\mathcal{T}\}$ corresponding to $\mathcal{H}^1(Z_n \rtimes Z_2^{\mathcal{T}}, \mathbb{Z}_a)$ satisfies the following algebraic conditions:

$$(U_R)^n = U_\mathcal{T} U_\mathcal{T}^* = U_R U_\mathcal{T} (U_R U_\mathcal{T})^* = 1. \tag{43}$$

Similar to $G_c = C_n$ case discussed earlier, in (42) the linear representation of n-fold rotation U_R is given by

$$U_R|\nu\rangle = u_{\nu_R}|\nu\rangle, \quad u_{\nu_R} = e^{2\pi i \frac{\nu_R}{a}}, \quad \nu_R = 0 \mod \frac{a}{(n,a)}. \tag{44}$$

While U_R is invariant under any gauge transformation on the basis vectors of the linear representation, this is not the case for antiunitary operator $\mathcal{T} = \mathcal{M}_\mathrm{v}^*$. Specifically under a gauge rotation by phase factor $e^{\frac{2\pi i}{a}}$ on all basis vectors, the linear representation of antiunitary operator $\mathcal{T}$ changes as

$$U_\mathcal{T}|\nu\rangle = u_{\nu_\mathcal{T}}|\nu\rangle, \quad |\nu\rangle \to e^{\frac{2\pi i}{a}}|\nu\rangle \Longrightarrow$$
$$U_\mathcal{T} = u_{\nu_\mathcal{T}} \to e^{\frac{2\pi i}{a}} u_{\nu_\mathcal{T}} (e^{-\frac{2\pi i}{a}})^* = u_{\nu_\mathcal{T}+2}. \tag{45}$$

This indicates that 1D G_0-SPT index $\nu_\mathcal{T}$ on each mirror plane is only well-defined modulo 2, leading to the $\mathbb{Z}_{(2,a)}$ factor in formula (42). This result has a straightforward physical interpretation: two 1D G_0-SPT phases of the same topological index can be merged from two sides into the mirror plane, hence changing the 1D topological index on the mirror plane by any even integer without closing the bulk gap.

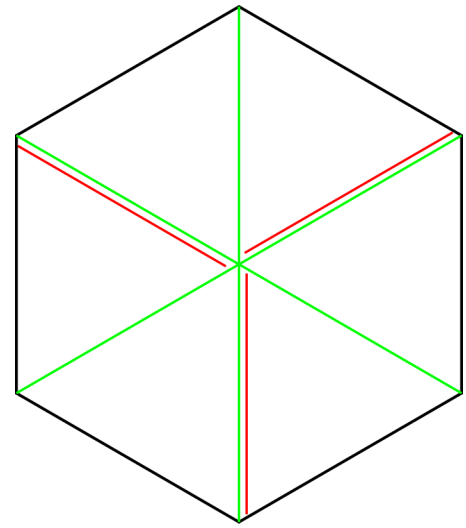

FIG. 4. Second-order SPT phases with $G_c = C_{3,\mathrm{v}}$ point-group symmetry, where each of the three C_3 domain walls is decorated by the same 1D G_0-SPT phase meeting at the rotation center, illustrated by red lines. Meanwhile, each mirror plane can also be decorated by another 1D G_0-SPT phase, labeled by the green lines.

Unlike in the previous $G_c = C_n$ case where the n copies of 1D G_0-SPT phases can be rotated by an arbitrary angle, here due to the presence of n mirror planes (related by C_n rotations), all 1D G_0-SPT phases are assigned to the mirror planes. As a result, as long as the corners of the finite system lie on the mirror planes, they will give rise to zero-energy corner modes protected by onsite G_0 symmetry. However as illustrated in Fig. 4, there are two different types of corners, terminating the green lines only versus terminating both green lines. These two types of corners generally support different types of projective representations of onsite symmetry G_0.

Finally, it is straightforward to show that the above classification and construction remain true for magnetic point group $G_c = C_n \rtimes Z_2^{\mathcal{M}_\mathrm{v}\mathcal{M}_\mathrm{h}\mathcal{T}}$, generated by rotation C_n around $\hat{z}$ axis and twofold antiunitary magnetic rotation $\mathcal{M}_\mathrm{v}\mathcal{M}_\mathrm{h}\mathcal{T}$ around an in-plane (such as $\hat{x}$) axis.

V. SECOND-ORDER SPT PHASES IN THREE DIMENSIONS

A. Classification

Second-order SPT phases in $d = 3$ are classified by $\mathcal{H}^1(G_c^*, \mathcal{H}^3(G_0, U(1)))$, i.e., linear representation of group G_c^* with coefficients valued in $\mathcal{H}^3(G_0, U(1))$. Physically, this means the building blocks for second-order SPT phases

in $d = 3$ are simply 2D G_0-SPT phases, classified by $\mathcal{H}^3(G_0, U(1))$ within the group cohomology framework.

Unlike 1D G_0-SPT phases which always form a finite Abelian group, 2D G_0-SPT phases can be an infinite Abelian group, as shown in the last line of Table II. Therefore, to classify second-order SPT phases in $d = 3$, we need to compute $\mathcal{H}^1(G_c^*, \mathbb{Z})$ in addition to knowledge of $\mathcal{H}^1(G_c^*, \mathbb{Z}_a)$ in (30)–(36). Below, we summarize $\mathcal{H}^1(G_c^*, \mathbb{Z})$ for all axial point groups and magnetic point groups G_c:

$$(C_n)^* \simeq Z_n, \quad \left(S_{2n}^{\mathcal{T}}\right)^* \simeq Z_{2n}, \quad \mathcal{H}^1(Z_n, \mathbb{Z}) = \mathbb{Z}_1; \tag{46}$$

$$(C_{n,\mathrm{v}})^* \simeq \left(C_n \rtimes Z_2^{\mathcal{M}_\mathrm{v}\mathcal{M}_\mathrm{h}\mathcal{T}}\right)^* \simeq Z_n \rtimes Z_2^{\mathcal{T}},$$
$$\mathcal{H}^1\left(Z_n \rtimes Z_2^{\mathcal{T}}, \mathbb{Z}\right) = \mathbb{Z}_2; \tag{47}$$

$$\left(C_{2n}^{\mathcal{T}}\right)^* \simeq (S_{2n})^* \simeq Z_{2n}^{\mathcal{T}}; \quad \mathcal{H}^1\left(Z_{2n}^{\mathcal{T}}, \mathbb{Z}\right) = \mathbb{Z}_2; \tag{48}$$

$$(D_{n,\mathrm{d}})^* \simeq \left(C_{2n}^{\mathcal{T}} \rtimes Z_2^{\mathcal{M}_\mathrm{v}}\right)^* \simeq Z_{2n}^{\mathcal{T}} \rtimes Z_2,$$
$$\mathcal{H}^1\left(Z_{2n}^{\mathcal{T}} \rtimes Z_2, \mathbb{Z}\right) = \mathbb{Z}_2; \tag{49}$$

$$(D_n)^* \simeq \left(C_n \rtimes Z_2^{\mathcal{M}_\mathrm{v}\mathcal{T}}\right)^* \simeq Z_n \rtimes Z_2,$$
$$\mathcal{H}^1(Z_n \rtimes Z_2, \mathbb{Z}) = \mathbb{Z}_1; \tag{50}$$

$$(C_{n,\mathrm{h}})^* \simeq \left(C_n \times Z_2^{\mathcal{I}}\right)^* \simeq Z_n \times Z_2^{\mathcal{T}},$$
$$\mathcal{H}^1\left(Z_n \times Z_2^{\mathcal{T}}, \mathbb{Z}\right) = \mathbb{Z}_2; \tag{51}$$

$$(D_{n,\mathrm{h}})^* \simeq (Z_n \rtimes Z_2) \times Z_2^{\mathcal{T}},$$
$$\mathcal{H}^1\left((Z_n \rtimes Z_2) \times Z_2^{\mathcal{T}}, \mathbb{Z}\right) = \mathbb{Z}_2. \tag{52}$$

Using relation (29) and results (30)–(36) and (46)–(52), we are able to compute $\mathcal{H}^1(G_c^*, \mathcal{H}^3(G_0, U(1)))$ for various onsite symmetry G_0. The classification of second-order SPT phases in $d = 3$ is summarized in Table II.

It is known that there are certain 2D short-range-entangled (SRE) bosonic phases (without intrinsic topological order) exhibiting chiral edge states [42,43], which are beyond the description of group cohomology classification. These SRE bosonic phases have an integer ($\mathbb{Z}$) classification, generated by the E_8 state with a chiral central charge $c_- = 8$.

One can also build higher-order SPT phases out of the bosonic E_8 states, as highlighted by the red color in Table II. The constructions for E_8 are analogous to the examples below for other chiral boson states, except that the hinges are decorated with E_8 phases. The bulk must be trivial and gapped, so the total chiral central charge in the bulk must vanish.

B. Examples

One physical signature of second-order SPT phases in $d = 3$ is the existence of gapless states on certain 1D hinges of the system. Below, we elucidate the procedure of constructing second-order SPT phases in $d = 3$ using the data of $\mathcal{H}^1(G_c^*, \mathcal{H}^3(G_0, U(1)))$, based on the decorated domain-wall construction where the building blocks are 2D G_0-SPT phases and bosonic E_8 states. We also show how this construction leads to gapless hinge states in 3D second-order SPT phases.

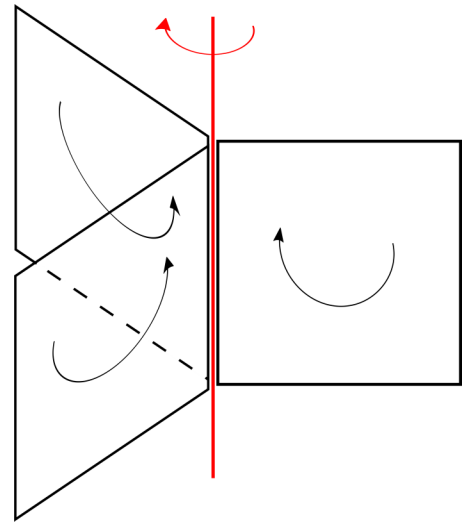

FIG. 5. Second-order SPT phases in $d = 3$ spatial dimensions, preserving C_3 rotational symmetry. Similar to $d = 2$ case in Fig. 3, they can be constructed by assigning the same 2D G_0-SPT phases on each C_3 domain wall.

1. $G_c = C_n$

In the simplest case of n-fold rotational symmetry $G_c = C_n$, the second-order SPT phases in 3D can be constructed by decorating each C_n domain wall by the same 2D G_0-SPT phase, as illustrated in Fig. 5. Similar to 2D cases discussed earlier, a gapped bulk provides strong constraints on the compatible 2D G_0-SPT phases, encoded in the following group cohomology formulas:

$$\mathcal{H}^1(Z_n, \mathbb{Z}_a) = \mathbb{Z}_{(n,a)} \tag{53}$$

and

$$\mathcal{H}^1(Z_n, \mathbb{Z}) = \mathbb{Z}_1. \tag{54}$$

This means if the 2D G_0-SPT phases has an integer classification, i.e., $\mathcal{H}^3(G_0, U(1)) = \mathbb{Z}$, none of these SPT phases are compatible to a gapped bulk when decorated on the C_n domain walls. On the other hand, if the 2D G_0-SPT phases form a finite group such as $\mathcal{H}^3(G_0, U(1)) = \mathbb{Z}_a$, only those with a topological index $\nu = 0 \mod \frac{a}{(n,a)}$ can lead to a gapped spectrum at the C_n rotation center, indicated by (41) discussed earlier. Similar to $d = 2$ cases in Sec. IV, these 2D G_0-SPT phases can be rotated together by an arbitrary angle around the C_n axis. Notice that 1D gapless hinge modes are not always present in a finite system: they only appear when the hinge intersects with the plane of each 2D G_0-SPT phase.

2. $G_c = C_{n,v}$

Considering point group $G_c = C_{n,\mathrm{v}}$ or magnetic point group $C_n \rtimes Z_2^{\mathcal{M}_\mathrm{v}\mathcal{M}_\mathrm{h}\mathcal{T}}$, the construction of associated second-order SPT phases in $d = 3$ is completely in parallel to $d = 2$ cases illustrated in Fig. 4. Specifically, two types of 2D G_0-SPT phases are assigned to each mirror plane: one type (red lines in Fig. 4) meeting at the C_n rotation center corresponds to the linear representation U_R of n-fold rotation generator R, the other type (green lines in Fig. 4) on each mirror plane corresponds to linear representation $U_{\mathcal{M}_\mathrm{v}}$ of mirror operation

$\mathcal{M}_\mathrm{v}$. They are constrained by the following compatibility conditions for a gapped bulk. When $\mathcal{H}^3(G_0, U(1))$, i.e., the classification of 2D G_0-SPT phases is a finite group, we have

$$\mathcal{H}^1\left(Z_n \rtimes Z_2^\mathcal{T}, \mathbb{Z}_a\right) = \mathbb{Z}_{(n,a)} \times \mathbb{Z}_{(2,a)}, \tag{55}$$

where $U_R \in \mathbb{Z}_{(n,a)}$ and $U_{\mathcal{M}_\mathrm{v}} \in \mathbb{Z}_{(2,a)}$, the same as discussed in Sec. IV for $d = 2$ case.

Meanwhile, if the classification of 2D G_0-SPT phases is an infinite group labeled, e.g., by an integer topological index $\nu \in \mathbb{Z}$, we have

$$\mathcal{H}^1\left(Z_n \rtimes Z_2^\mathcal{T}, \mathbb{Z}\right) = \mathbb{Z}_2, \tag{56}$$

where $U_R \equiv u_0 \in \mathbb{Z}_1$ and $U_{\mathcal{M}_\mathrm{v}} = u_{\nu_{\mathcal{M}_\mathrm{v}} \mod 2} \in \mathbb{Z}_2$. Physically, for the C_n rotation center to be gapped, one can only assign a trivial 2D phase on each C_n domain wall, corresponding to the trivial representation $U_R \equiv u_0$. On the other hand, each mirror plane can be decorated by any 2D G_0-SPT phase with topological index $\nu_{\mathcal{M}_\mathrm{v}}$. The second-order SPT phase is only characterized by the parity of topological index $\nu_{\mathcal{M}_\mathrm{v}} \mod 2$ since a pair of the same 2D G_0-SPT phases can always be merged onto the mirror plane without closing the bulk gap.

As shown in Fig. 4, the gapless hinge states will appear in a finite system as long as the hinge lies within a mirror plane. The gapless 1D modes on the two opposite hinges of the same mirror plane are generally different from each other, as illustrated by the green hinges versus green-plus-red hinges in Fig. 4.

3. $G_c = S_{2n}$ or $G_c = C_{2n}^\mathcal{T}$

Point group S_{2n} is generated by a $\frac{\pi}{n}$ rotation R along $\hat{z}$ axis followed by a mirror $\mathcal{M}_\mathrm{h}$ with respect to [001] plane:

$$S_{2n} = \{\mathcal{S}^i | 1 \leqslant i \leqslant 2n\}, \quad \mathcal{S} = R\mathcal{M}_\mathrm{h} \Longrightarrow \mathcal{S}^{2n} = 1. \tag{57}$$

Operation $\mathcal{S}$ is usually referred to as an improper rotation or a rotoreflection. For both point group S_{2n} and magnetic point group $C_{2n}^\mathcal{T}$ defined below

$$C_{2n}^\mathcal{T} \equiv \{(R\mathcal{T})^i | 1 \leqslant i \leqslant 2n\} \tag{58}$$

they share the same classification for second-order SPT phases since

$$(S_{2n})^* \simeq \left(C_{2n}^\mathcal{T}\right)^* \simeq Z_{2n}^\mathcal{T}, \tag{59}$$

where $Z_{2n}^\mathcal{T}$ is generated by an antiunitary operator of rank $2n$. The following group cohomology formulas determine the classification of second-order SPT phases with S_{2n} or $C_{2n}^\mathcal{T}$ symmetry:

$$\mathcal{H}^1\left(Z_{2n}^\mathcal{T}, \mathbb{Z}_a\right) = \mathbb{Z}_{(2,a)} \tag{60}$$

and

$$\mathcal{H}^1\left(Z_{2n}^\mathcal{T}, \mathbb{Z}\right) = \mathbb{Z}_2. \tag{61}$$

They are determined by solving the following conditions for linear representation $U_\mathcal{S} \in \mathbb{Z}_a, \mathbb{Z}$:

$$U_\mathcal{S} U_\mathcal{S}^* = 1. \tag{62}$$

They can be understood similar to the mirror symmetry $\mathcal{M}_\mathrm{v}$ in the $G_c = C_{n,\mathrm{v}}$ case, where we have $U_\mathcal{S} = u_{\nu_\mathcal{S} \mod 2}$ and the topological index $\nu_\mathcal{S}$ of the 2D G_0-SPT phase is only well defined modulo 2. To construct these S_{2n}-symmetric second-order SPT phases, we decorate each $\mathcal{S}$ domain wall by a 2D G_0-SPT phase with topological index $\nu_\mathcal{S} \mod 2$, in a staggered fashion as shown in Fig. 6. Again, we can always merge two identical G_0-SPT phases into each $\mathcal{S}$ domain wall without closing the bulk gap, which will change the topological index of 2D G_0 SPT phase on this $\mathcal{S}$ domain wall by an even integer. This physically explains why the topological index for the 2D G_0-SPT phase $\nu_\mathcal{S}$ decorated on each $\mathcal{S}$ domain wall is only defined modulo 2, manifested in the $\mathbb{Z}_{(2,a)}$ and $\mathbb{Z}_2$ classifications in (60) and (61).

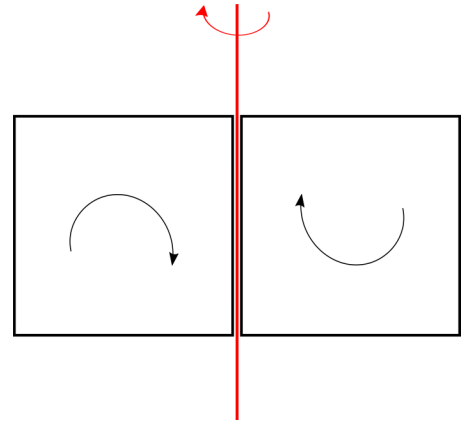

FIG. 6. Second-order SPT phases with point-group symmetry S_2 or magnetic point group $C_2^\mathcal{T} = \{(R\mathcal{T})^i | i = 0, 1\}$.

4. $G_c = D_{n,d} \equiv S_{2n} \rtimes Z_2^{\mathcal{M}_\mathrm{v}}$ or $C_{2n}^\mathcal{T} \rtimes Z_2^{\mathcal{M}_\mathrm{v}}$

Point group $D_{n,\mathrm{d}}$ is generated by $2n$-fold rotoreflection $\mathcal{S} = R\mathcal{M}_\mathrm{h}$ around $\hat{z}$ axis as discussed earlier in $G_c = S_{2n}$ case, and a mirror plane $\mathcal{M}_\mathrm{v}$ parallel to $\hat{z}$ axis. The group $D_{n,\mathrm{d}}$ can be summarized as

$$D_{n,\mathrm{d}} = \{\mathcal{S}^{i_s}(R_2)^{i_2} | 1 \leqslant i_s \leqslant 2n, 1 \leqslant i_2 \leqslant 2\}, \tag{63}$$

where we defined $R_2 \equiv \mathcal{S}\mathcal{M}_\mathrm{v}$ as a twofold rotation along an in-plane axis (colored red in Fig. 7), so that $\mathcal{S}^{2n} = (\mathcal{S}\mathcal{M}_\mathrm{v})^2 = 1$. The linear representation $\mathcal{H}^1(G_c^*, \mathcal{H}^3(G_0, U(1))) = \{U_\mathcal{S}, U_{R_2} \in \mathcal{H}^3(G_0, U(1))\}$ must satisfy the following algebraic conditions:

$$U_\mathcal{S} U_\mathcal{S}^* = 1, \tag{64}$$

$$(U_{R_2})^2 = 1, \tag{65}$$

$$U_{R_2} U_\mathcal{S} (U_{R_2} U_\mathcal{S})^* = 1. \tag{66}$$

If 2D G_0-SPT phases have a finite classification such as $\mathcal{H}^3(G_0, U(1)) = \mathbb{Z}_a$, the linear representations are classified as

$$\mathcal{H}^1\left(Z_{2n}^\mathcal{T} \rtimes Z_2, \mathbb{Z}_a\right) = \mathbb{Z}_{(2,a)}^2 \tag{67}$$

given by

$$U_\mathcal{S} = e^{\frac{2\pi \mathrm{i}}{a} \nu_\mathcal{S}}, \quad \nu_\mathcal{S} \simeq \nu_\mathcal{S} + 2, \tag{68}$$

$$U_{R_2} = e^{\frac{2\pi \mathrm{i}}{a} \nu_{R_2}}, \quad 2\nu_{R_2} = 0 \mod a, \tag{69}$$

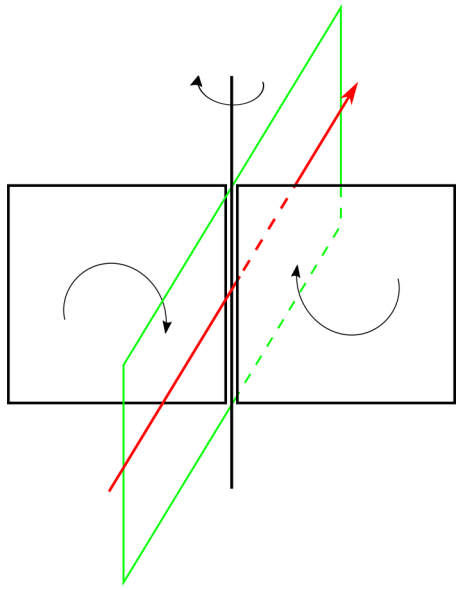

FIG. 7. Second-order SPT phases with point-group symmetry $D_{n,\mathrm{d}}$. There is a twofold rotoreflection axis along $\hat{z}$ axis and a twofold in-plane axis (colored red). 2D G_0-SPT phases with topological index $\mathcal{S}$ are decorated on each mirror plane, while 2D G_0-SPT phases with index ν_{R_2} are decorated on vertical planes crossing each R_2 axis.

where $\nu_{\mathcal{S}}$ and ν_{R_2} are the topological indices of 2D G_0-SPT phases decorated on $\mathcal{S}$ and R_2 domain walls, respectively.

If 2D G_0-SPT phases have an infinite classification such as $\mathcal{H}^3(G_0, U(1)) = \mathbb{Z}$, we have

$$\mathcal{H}^1\left(Z_{2n}^{\mathcal{T}} \rtimes Z_2, \mathbb{Z}\right) = \mathbb{Z}_2, \tag{70}$$

where

$$\nu_{\mathcal{S}} = 0, 1 \simeq \nu_{\mathcal{S}} + 2, \quad \nu_{R_2} = 0. \tag{71}$$

Physically, the 2D G_0-SPT phases decorated on each $\mathcal{S}$ domain wall (chosen to lie within a mirror plane) have topological indices $\nu_{\mathcal{S}} = 0, 1$ defined modulo 2, for the same reason described previously in $G_c = S_{2n}$ case. They are illustrated by black color in Fig. 7. On the other hand, the topological index $\nu_{R_2} \simeq -\nu_{R_2}$ decorated on each R_2 domain wall must be nonchiral, and hence must be trivial when $\mathcal{H}^3(G_0, U(1)) = \mathbb{Z}$. These ν_{R_2}-indexed 2D G_0-SPT phases are decorated on vertical planes parallel to each R_2 axis, as illustrated by the green plane in Fig. 7.

Clearly, the hinges of a finite system can host 1D gapless modes for these second-order SPT phases, if the hinge lies within a mirror plane or a vertical plane containing one twofold axis. Generally, the gapless modes on these two types of hinges will be different.

5. $G_c = D_{n,h} \equiv C_{n,v} \times Z_2^{\mathcal{M}_h}$

Finally, we consider the following point group:

$$D_{n,\mathrm{h}} = \{(R_z)^{i_n}(R_x)^{i_2}(\mathcal{M}_{\mathrm{h}})^{i_{\mathcal{M}}} | i_n \in Z_n, i_2, i_{\mathcal{M}} \in Z_2\}. \tag{72}$$

As shown in Fig. 8, it is generated by n-fold rotation R_z along $\hat{z}$ axis, twofold rotation R_x along $\hat{x}$ axis and mirror $\mathcal{M}_{\mathrm{h}}$ with respect to the x-y (or [001]) plane (colored in blue in Fig. 8).

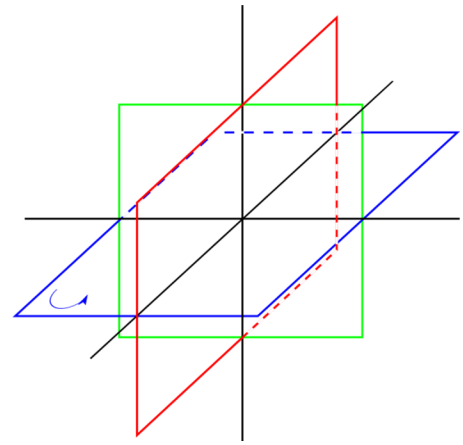

FIG. 8. Second-order SPT phases with $D_{n,\mathrm{h}}$ point-group symmetry. 2D G_0-SPT phases with topological indices ν_{R_z}, ν_{R_x}, and $\nu_{\mathcal{M}_{\mathrm{h}}}$ are assigned to red, green, and blue mirror planes, respectively.

Its linear representation $\{U_{R_x}, U_{R_z}, U_{\mathcal{M}_{\mathrm{h}}} \in \mathcal{H}^3(G_0, U(1))\} \in \mathcal{H}^1(D_{n,\mathrm{h}}^*, \mathcal{H}^3(G_0, U(1)))$ satisfies the following conditions:

$$\left(U_{R_z}\right)^n = \left(U_{R_x}\right)^2 = \left(U_{R_x}U_{R_z}\right)^2 = 1, \tag{73}$$

$$U_{\mathcal{M}_{\mathrm{h}}}U_{\mathcal{M}_{\mathrm{h}}}^* = 1, \tag{74}$$

$$U_{R_z}U_{\mathcal{M}_{\mathrm{h}}}\left(U_{R_z}U_{\mathcal{M}_{\mathrm{h}}}\right)^* = 1, \tag{75}$$

$$U_{R_x}U_{\mathcal{M}_{\mathrm{h}}}\left(U_{R_x}U_{\mathcal{M}_{\mathrm{h}}}\right)^* = 1. \tag{76}$$

When 2D G_0-SPT phases have a finite classification, e.g., $\mathcal{H}^3(G_0, U(1)) = \mathbb{Z}_a$ we have

$$\mathcal{H}^1\left((Z_n \rtimes Z_2) \times Z_2^{\mathcal{T}}, \mathbb{Z}_a\right) = \mathbb{Z}_{(n,a,2)} \times \mathbb{Z}_{(2,a)}^2, \tag{77}$$

where

$$U_{R_z} = e^{\frac{2\pi \mathrm{i}}{a}\nu_{R_z}} \in \mathbb{Z}_{(n,a,2)}, \quad n\nu_{R_z} = 2\nu_{R_z} = 0 \mod a, \tag{78}$$

$$U_{R_x} = e^{\frac{2\pi \mathrm{i}}{a}\nu_{R_x}} \in \mathbb{Z}_{(a,2)}, \quad 2\nu_{R_x} = 0 \mod a, \tag{79}$$

$$U_{\mathcal{M}_{\mathrm{h}}} = e^{\frac{2\pi \mathrm{i}}{a}\nu_{\mathcal{M}_{\mathrm{h}}}} \in \mathbb{Z}_{(a,2)}, \quad \nu_{\mathcal{M}_{\mathrm{h}}} = 0, 1 \mod 2. \tag{80}$$

Meanwhile, if 2D G_0-SPT phases have an infinite classification, e.g., $\mathcal{H}^3(G_0, U(1)) = \mathbb{Z}$ we have

$$\mathcal{H}^1\left((Z_n \rtimes Z_2) \times Z_2^{\mathcal{T}}, \mathbb{Z}\right) = \mathbb{Z}_2, \tag{81}$$

where

$$\nu_{R_z} = \nu_{R_x} \equiv 0, \quad \nu_{\mathcal{M}_{\mathrm{h}}} = 0, 1 \mod 2 \in \mathbb{Z}_2. \tag{82}$$

Physically, both R_z and R_x domain walls must be decorated with nonchiral 2D G_0-SPT phases due to the mirror symmetry $\mathcal{M}_{\mathrm{h}}$, as denoted by red (ν_{R_z}) and green (ν_{R_x}) in Fig. 8. Meanwhile, the $\mathcal{M}_{\mathrm{h}}$ mirror plane can be decorated with a (possibly chiral) 2D G_0-SPT phase with index $\nu_{\mathcal{M}_{\mathrm{h}}}$, as denoted by blue in Fig. 8.

From the above construction, we can see that there are three types of hinges hosting different gapless 1D modes in the system: (i) 1D hinge modes lying in the mirror $\mathcal{M}_{\mathrm{h}}$ plane (colored in blue) has topological index $\nu_{\mathcal{M}_{\mathrm{h}}}$; (ii) 1D hinge modes lying in vertical mirror $R_x\mathcal{M}_{\mathrm{h}}$ plane (colored in green)

has index ν_{R_x}; (iii) 1D hinge modes lying in vertical mirror $R_z R_x \mathcal{M}_\mathrm{h}$ plane (colored in red) has index ν_{R_z}.

VI. THIRD-ORDER SPT PHASES IN THREE DIMENSIONS

The third-order SPT phases in $d = 3$ are classified by second group cohomology $\mathcal{H}^2(G_c^*, \mathcal{H}^2(G_0, U(1)))$ whose coefficients take value in $\mathcal{H}^2(G_0, U(1))$. Physically, they can be constructed by stacking 1D G_0-SPT phases, i.e., elements of $\mathcal{H}^2(G_0, U(1))$, in a way which preserves (magnetic) crystalline symmetry G_c. Specifically, as previously discussed in the decorated domain-wall picture in Sec. III C, they can all be built by decorating 1D intersections of domain walls with 1D G_0-SPT phases. Below, we first classify these third-order SPT phases in $d = 3$ dimensions, for various onsite symmetry G_0 and (magnetic) point group G_c. Then, we illustrate how to explicitly construct these states in a few examples.

A. Classification

To compute the group cohomology $\mathcal{H}^2(G_c^*, \mathcal{H}^2(G_0, U(1)))$ for third-order SPT phases, we first notice that the classification of 1D G_0-SPT phases always form a finite discrete Abelian group, which are products of the cyclic group $\mathbb{Z}_a$ for a finite $a \in \mathbb{Z}$. Therefore, according to relation (29), we only need to know $\mathcal{H}^2(G_c^*, \mathbb{Z}_a)$ in order to compute $\mathcal{H}^2(G_c^*, \mathcal{H}^2(G_0, U(1)))$.

Below, we list the results for various point groups and magnetic point groups G_c:

$$(C_n)^* \simeq Z_n, \quad \left(S_{2n}^{\mathcal{T}}\right)^* \simeq Z_{2n}, \quad \mathcal{H}^2(Z_n, \mathbb{Z}_a) = \mathbb{Z}_{(n,a)}; \tag{83}$$

$$(C_{n,\mathrm{v}})^* \simeq \left(C_n \rtimes Z_2^{\mathcal{M}_\mathrm{v}\mathcal{M}_\mathrm{h}\mathcal{T}}\right)^* \simeq Z_n \rtimes Z_2^{\mathcal{T}},$$
$$\mathcal{H}^2\left(\left(C_n \rtimes Z_2^{\mathcal{M}_\mathrm{v}\mathcal{M}_\mathrm{h}\mathcal{T}}\right)^*, \mathbb{Z}_a\right) = \mathbb{Z}_{(n,a,2)} \times \mathbb{Z}_{(n,a)} \times \mathbb{Z}_{(2,a)}; \tag{84}$$

$$\mathcal{H}^2((C_{n,\mathrm{v}})^*, \mathbb{Z}_a) = \mathbb{Z}_{(n,a)} \times \mathbb{Z}_{(n,a,2)} \times \mathbb{Z}_{(2,a)}; \tag{85}$$

$$\left(C_{2n}^{\mathcal{T}}\right)^* \simeq (S_{2n})^* \simeq Z_{2n}^{\mathcal{T}}; \quad \mathcal{H}^2\left(Z_{2n}^{\mathcal{T}}, \mathbb{Z}_a\right) = \mathbb{Z}_{(2,a)}; \tag{86}$$

$$(D_{n,\mathrm{d}})^* \simeq \left(C_{2n}^{\mathcal{T}} \rtimes Z_2^{\mathcal{M}_\mathrm{v}}\right)^* \simeq Z_{2n}^{\mathcal{T}} \rtimes Z_2,$$
$$\mathcal{H}^2((D_{n,\mathrm{d}})^*, \mathbb{Z}_a) = \mathbb{Z}_{(2,a)}^2 \times \mathbb{Z}_{(2,a)}; \tag{87}$$

$$\mathcal{H}^2\left(\left(C_{2n}^{\mathcal{T}} \rtimes Z_2^{\mathcal{M}_\mathrm{v}}\right)^*, \mathbb{Z}_a\right) = \mathbb{Z}_{(2,a)} \times \mathbb{Z}_{(2,a)}^2; \tag{88}$$

$$(D_n)^* \simeq \left(C_n \rtimes Z_2^{\mathcal{M}_\mathrm{v}\mathcal{T}}\right)^* \simeq Z_n \rtimes Z_2,$$
$$\mathcal{H}^2((D_n)^*, \mathbb{Z}_a) = \mathbb{Z}_{(n,a,2)} \times \mathbb{Z}_{(a,2)}^2; \tag{89}$$

$$\mathcal{H}^2\left(\left(C_n \rtimes Z_2^{\mathcal{M}_\mathrm{v}\mathcal{T}}\right)^*, \mathbb{Z}_a\right) = \mathbb{Z}_{(n,a,2)} \times \mathbb{Z}_{(a,2)}^2;$$
$$(C_{n,\mathrm{h}})^* \simeq \left(C_n \times Z_2^{\mathcal{I}}\right)^* \simeq Z_n \times Z_2^{\mathcal{T}}, \tag{90}$$

$$\mathcal{H}^2\left(Z_n \times Z_2^{\mathcal{T}}, \mathbb{Z}_a\right) = \mathbb{Z}_{(n,a,2)} \times \mathbb{Z}_{(2,a)} \times \mathbb{Z}_{(2,a)};$$
$$(D_{n,\mathrm{h}})^* \simeq (Z_n \rtimes Z_2) \times Z_2^{\mathcal{T}}, \tag{91}$$

$$\mathcal{H}^2((D_{n,\mathrm{h}})^*, \mathbb{Z}_a) = \mathbb{Z}_{(n,a,2)}^2 \times \mathbb{Z}_{(2,a)} \times \mathbb{Z}_{(2,a)}^3; \tag{92}$$

$$T^* \simeq A_4 = (Z_2 \times Z_2) \rtimes Z_3, \quad \mathcal{H}^2(A_4, \mathbb{Z}_a) = \mathbb{Z}_{(3,a)} \times \mathbb{Z}_{(2,a)}; \tag{93}$$

$$(T_\mathrm{h})^* \simeq A_4 \times Z_2^{\mathcal{T}}, \quad \mathcal{H}^2\left(A_4 \times Z_2^{\mathcal{T}}, \mathbb{Z}_a\right) = \mathbb{Z}_{(2,a)}^2 \times \mathbb{Z}_{(2,a)}. \tag{94}$$

They are projective representations of group G_c^* with coefficients valued in $\mathbb{Z}_a$. Using these results and relation (29), we obtain the classification of third-order SPT phases for these (magnetic) point groups G_c and various onsite symmetry G_0, as summarized in Table III.

B. Examples

1. $G_c = C_n$

First, we consider point group C_n, generated by rotation R along, e.g., the $\hat{z}$ axis. Its second group cohomology is classified by

$$\mathcal{H}^2(Z_n, \mathbb{Z}_a) = \mathbb{Z}_{(n,a)} \tag{95}$$

which can be understood as follows. As described in Sec. III C, the second group cohomology $\mathcal{H}^2(Z_n, \mathbb{Z}_a)$ are projective representations $\{\omega(g, h) \in \mathbb{Z}_a | g, h \in Z_n\}$ valued in $\mathbb{Z}_a = \{e^{\frac{2\pi \mathrm{i}}{a}\nu} | \nu \in \mathbb{Z}\}$, defined below:

$$U_g U_h^{s(g)} = \omega(g, h) U_{gh}, \tag{96}$$

$$\omega(g, h)\omega(gh, k) = \omega(g, hk)\omega^{s(g)}(h, k). \tag{97}$$

For our group $(C_n)^* \simeq Z_n$ with $R^n = 1$, we have

$$(U_R)^n = \omega_{C_n} 1, \quad \omega_{C_n} = \prod_{i=1}^{n-1} \omega(R, R^i) = e^{\frac{2\pi \mathrm{i}}{a}\nu_{C_n}} \in \mathbb{Z}_a \tag{98}$$

since $U_1 \equiv 1$. Notice that we can always redefine the symmetry operation by an extra phase factor valued in $\mathbb{Z}_a$,

$$U_R \to e^{\frac{2\pi \mathrm{i}}{a}} U_R, \tag{99}$$

which leads to equivalence relation

$$\nu_{C_n} \simeq \nu_{C_n} + n \mod a \in \mathbb{Z}_{(n,a)}, \tag{100}$$

where (n, a) is the greatest common divisor of integers n and a. This leads to the second group cohomology formula (95).

Physically, as argued in Sec. III C, we decorate each C_n rotational axis by a 1D G_0-SPT phase with topological index ν_{C_n}. Notice that we can always merge n copies of the same 1D G_0-SPT phases into the rotational axis in a C_n-symmetric manner, without closing the bulk gap. This physically explains the equivalence relation (100).

Unlike second-order SPT phases in $d = 3$ which hosts gapless 1D hinge states, third-order SPT phases in $d = 3$ only support gapless zero modes at the corners of certain finite systems, which carry projective representation of onsite symmetry G_0. For example, here for point group $G_c = C_n$ or magnetic point group $G_c = S_{2n}^{\mathcal{T}} = \{(\mathcal{S}\mathcal{T})^i | 1 \leqslant i \leqslant 2n\}$, there will be protected zero modes at every corner of the finite system lying on a C_n rotatonal axis.

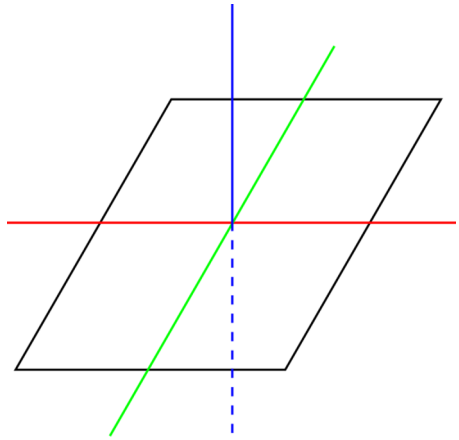

FIG. 9. Third-order SPT phases with magnetic point-group symmetry $C_n \rtimes Z_2^{\mathcal{M}_v \mathcal{M}_h \mathcal{T}}$ with $n = 2$. The topological indices of 1D G_0-SPT phases are labeled by ν_R (colored blue, along n-fold vertical rotation axis R), $\nu_{\mathcal{C}}$ (colored red, along twofold horizontal magnetic rotation axis $\mathcal{C}$), and $\nu_{R\mathcal{C}}$ (colored green, along twofold horizontal magnetic rotation axis $R\mathcal{C}$).

2. $G_c = C_n \rtimes Z_2^{\mathcal{M}_v \mathcal{M}_h \mathcal{T}}$ and $C_{n,v}$

Next, we consider magnetic point group $C_n \rtimes Z_2^{\mathcal{M}_v \mathcal{M}_h \mathcal{T}}$ and point group $C_{n,v}$, which share the same

$$G_c^* \simeq Z_2 \rtimes Z_2^{\mathcal{T}}. \tag{101}$$

Take magnetic point group $G_c = C_n \rtimes Z_2^{\mathcal{M}_v \mathcal{M}_h \mathcal{T}}$ for example: generated by n-fold vertical rotation R and twofold horizontal magnetic rotation axis $\mathcal{C} \equiv \mathcal{M}_v \mathcal{M}_h \mathcal{T}$, it is defined by the following algebraic relations:

$$R^n = \mathcal{C}^2 = (R\mathcal{C})^2 = 1, \tag{102}$$

where both $\mathcal{C}$ and $R\mathcal{C}$ correspond to in-plane (horizontal) twofold magnetic rotation axes. Its projective representation

$$\mathcal{H}^2\left(Z_n \rtimes Z_2^{\mathcal{T}}, \mathbb{Z}_a\right) = \mathbb{Z}_{(n,a,2)} \times \mathbb{Z}_{(n,a)} \times \mathbb{Z}_{(2,a)} \tag{103}$$

is characterized by $\mathbb{Z}_a$-valued factors

$$(U_R)^n = \omega_{C_n} \equiv e^{\frac{2\pi \mathrm{i}}{a} \nu_{C_n}}, \tag{104}$$

$$U_{\mathcal{C}} U_{\mathcal{C}}^* = \omega_{\mathcal{C}} = e^{\frac{2\pi \mathrm{i}}{a} \nu_{\mathcal{C}}}, \tag{105}$$

$$U_R U_{\mathcal{C}} (U_R U_{\mathcal{C}})^* = \omega_{R\mathcal{C}} = e^{\frac{2\pi \mathrm{i}}{a} (\nu_{R\mathcal{C}} + \nu_{\mathcal{C}})}. \tag{106}$$

It is straightforward to show that the solutions to the factors are

$$\nu_{C_n} \simeq \nu_{C_n} + n \mod a \in \mathbb{Z}_{(n,a)}, \tag{107}$$

$$2\nu_{\mathcal{C}} = 0 \mod a \Longrightarrow \nu_{\mathcal{C}} \in \mathbb{Z}_{(n,a,2)}, \tag{108}$$

$$2\nu_{R\mathcal{C}} = n\nu_{R\mathcal{C}} = 0 \mod a \Longrightarrow \nu_{R\mathcal{C}} \in \mathbb{Z}_{(n,a,2)}, \tag{109}$$

as shown earlier in (84). Physically, they correspond to the topological index of 1D G_0-SPT phases decorated on the C_n rotation axis (ν_{C_n}, colored blue in Fig. 9), on each horizontal $\mathcal{C}$ axis ($\nu_{\mathcal{C}}$, colored red in Fig. 9), and on each horizontal $R\mathcal{C}$ axis ($\nu_{R\mathcal{C}}$, colored green in Fig. 9), as shown in Fig. 9.

Clearly, there are robust corner states at each intersection of the surface with the three types of rotation axes: vertical n-fold rotation R, horizontal twofold magnetic rotation $\mathcal{C}$ and $R\mathcal{C}$. All these corner states are protected by onsite symmetry G_0 and are robust against disorders and crystal distortions.

Compared to magnetic point group $C_n \rtimes Z_2^{\mathcal{M}_v \mathcal{M}_h \mathcal{T}}$, the point group $G_c = C_n$ case is different. In addition to n-fold vertical rotation axis R, it also has vertical mirror planes $\mathcal{M}_v$ and $R\mathcal{M}_v$. Although the Künneth formula (85) yields the same outcome as the magnetic point group in (84), the factors have different meanings. While ν_{C_n} still labels the topological index of 1D G_0-SPT phase decorated on the vertical C_n rotation axis, $\nu_{\mathcal{C}}$ and $\nu_{R\mathcal{C}}$ correspond to weak crystalline SPT indices. They characterize whether each 2D mirror plane, $\mathcal{M}_v$ and $R\mathcal{M}_v$, are 2D SPT phases protected by mirror and G_0 symmetries. Although there can be gapless boundary states if mirror symmetry is preserved by the surface, they are generally not stable against perturbations breaking the mirror symmetry on the surface.

3. $G_c = T$

Point group T is generated by twofold rotations $R_{y,z}$ along $\hat{y}$ and $\hat{z}$ axes, as well as threefold rotations R_3 along (111) axis:

$$T \equiv \left\{ R_y^{i_y} R_z^{i_z} R_3^{i_3} \middle| i_{y,z} \in Z_2,\ i_3 \in Z_3 \right\}. \tag{110}$$

The group multiplication rules are set by the following algebraic identities:

$$(R_y)^2 = (R_z)^2 = (R_y R_z)^2 = (R_3)^2 = 1, \tag{111}$$

$$R_3 R_z R_3^{-1} = R_y R_z, \quad R_3 R_y R_3^{-1} = R_z. \tag{112}$$

Its projective representation is determined by the following phase factors:

$$\left(U_{R_y}\right)^2 = \left(U_{R_z}\right)^2 = \left(U_{R_y} U_{R_z}\right) = \omega_2 = e^{\frac{2\pi \mathrm{i}}{a} \nu_2} \in \mathbb{Z}_a, \tag{113}$$

$$\left(U_{R_3}\right)^3 = \omega_3 = e^{\frac{2\pi \mathrm{i}}{a} \nu_3} \in \mathbb{Z}_a. \tag{114}$$

It is straightforward to show that

$$\nu_3 \simeq \nu_3 + 3 \mod a \Longrightarrow \nu_3 \in \mathbb{Z}_{(a,3)}, \tag{115}$$

$$\nu_2 = -\nu_2 \mod a \Longrightarrow \nu_2 \in \mathbb{Z}_{(a,2)}, \tag{116}$$

leading to the group cohomology classification

$$\mathcal{H}^2(T^* \simeq A_4, \mathbb{Z}_a) = \mathbb{Z}_{(3,a)} \times \mathbb{Z}_{(2,a)}. \tag{117}$$

As shown in Fig. 10, the T-symmetric third-order SPT phases are constructed by decorating all four of the threefold axes (green in Fig. 10) by 1D G_0-SPT phases with topological index $\nu_3 \in \mathbb{Z}_{(3,a)}$, and decorating all three of the twofold axes (red in Fig. 10) by 1D G_0-SPT phases with topological index $\nu_2 \in \mathbb{Z}_{(2,a)}$.

Now, we discuss G_0 symmetry-protected corner states in the system. If the surface intersects with any of the twofold or threefold axes, it will host gapless corner modes protected by onsite symmetry G_0 at the intersection. Generally the projective representations for corners on the twofold and threefold axes will be different. Take a spin-1 system with $G_0 = SO(3)$ symmetry, for example, there will only be gapless spin-$\frac{1}{2}$

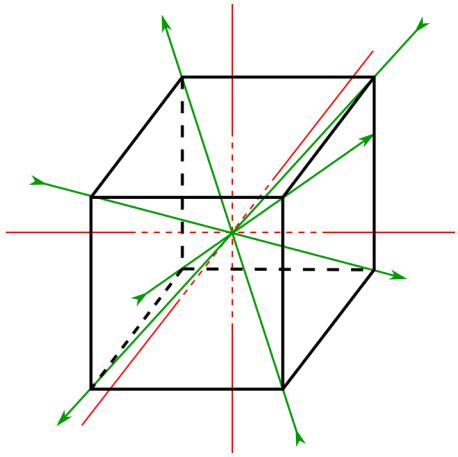

FIG. 10. Third-order SPT phases with point-group symmetry T. They are constructed by decorating the four threefold axes (green) with 1D G_0-SPT phases with topological index ν_3, and the three twofold axes (red) with topological index ν_2.

modes at each corner on the $\hat{x}$, $\hat{y}$, and $\hat{z}$ axes, but not on the (111) axis.

4. $G_c = T_h = T \times Z_2^{\mathcal{I}}$

Finally, we consider the point group T_h, which is a direct product of group T and the rank-2 group $Z_2^{\mathcal{I}}$ generated by inversion $\mathcal{I}$. In addition to algebraic relations (111) and (112), we also have

$$\mathcal{I}^2 = 1, \tag{118}$$

$$\mathcal{I} R_\alpha \mathcal{I}^{-1} = R_\alpha, \quad \alpha = y, z, 3. \tag{119}$$

This leads to three more phase factors, in addition to $\omega_{2,3}$ considered in $G_c = T$ case:

$$U_{\mathcal{I}} U_{\mathcal{I}}^* = \omega_1 = e^{\frac{2\pi \mathrm{i}}{a}\nu_1}, \tag{120}$$

$$U_{\mathcal{I}} U_{R_{y,z}}^* U_{\mathcal{I}}^{-1} U_{R_{y,z}}^{-1} = \omega_4 = e^{\frac{2\pi \mathrm{i}}{a}\nu_4}, \tag{121}$$

$$U_{\mathcal{I}} U_{R_3}^* U_{\mathcal{I}}^{-1} U_{R_3}^{-1} = \omega_5 = e^{\frac{2\pi \mathrm{i}}{a}\nu_5}. \tag{122}$$

It is straightforward to show that $\omega_{4,5} \equiv 1$, and

$$2\nu_i = 0 \mod a \Longrightarrow \nu_i \in \mathbb{Z}_{(2,a)}, \quad i = 1, 2, 3. \tag{123}$$

This results in the second group cohomology classification

$$\mathcal{H}^2\left(T_{\mathrm{h}}^* \simeq A_4 \times Z_2^{\mathcal{T}}, \mathbb{Z}_a\right) = \mathbb{Z}_{(2,a)}^3. \tag{124}$$

Physically similar to $G_c = T$ case discussed earlier, $\nu_{2,3}$ still correspond to the topological indices of 1D G_0-SPT phases, assigned along the two types of high-symmetry axes (and their symmetry-related partners) colored by red (with index ν_2) and green (with index ν_3) as shown in Fig. 11. As a result, if the surface of an open system intersects with one of these axes, it will host gapless corner modes protected by onsite symmetry G_0. A difference between this case and the previous $G_c = T$ example is that due to inversion symmetry, each 1D SPT phase decorated along a high-symmetry axis must be its own inverse phase, leading to $\omega_i = \omega_i^* = \pm 1$.

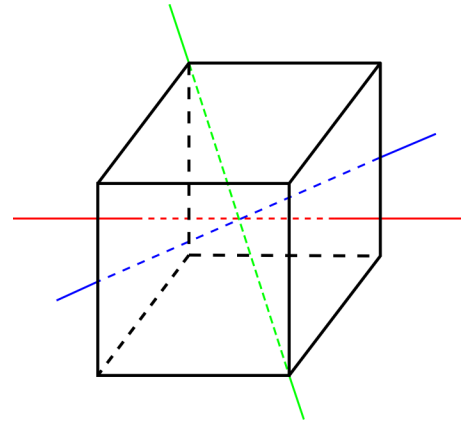

FIG. 11. Third-order SPT phases with point-group symmetry T_h, classified by three topological invariants $\nu_{1,2,3}$. Among them, $\nu_{2,3}$ correspond to the topological indices of 1D G_0-SPT phases along the two types of high-symmetry axes colored by red and green, while $\nu_1 + \nu_2$ labels whether each mirror plane (perpendicular to red axis) is a 2D SPT protected by both mirror and onsite symmetry G_0.

Meanwhile, ν_1 has a slightly different physical meaning. Notice that there are three mirror planes associated with mirror reflection symmetry $\mathcal{M}_\alpha = \mathcal{I} R_\alpha$ for $\alpha = x, y, z$. Since each mirror symmetry serves as an onsite Z_2 symmetry within its 2D mirror plane, the projective representation of the mirror symmetry

$$U_{\mathcal{M}_\alpha} U_{\mathcal{M}_\alpha}^* = U_{\mathcal{I}} U_{R_\alpha}^* U_{\mathcal{I}}^* U_{R_\alpha} = \omega_1 \omega_2 \in \mathbb{Z}_{(2,a)} \tag{125}$$

corresponds to whether each 2D mirror plane is a SPT phase protected by both Z_2 mirror symmetry and onsite symmetry G_0. In other words, $\omega_1\omega_2 = \pm 1$ labels whether the mirror domain wall within each mirror plane is decorated by a 1D G_0-SPT phase or not. Therefore, $\omega_1\omega_2$ is an index for weak crystalline SPT phases, and generally does not host corner/hinge modes robust against small mirror-breaking perturbations.

VII. DISCUSSIONS

In summary, to understand the HOSPT phases of interacting bosons with robust symmetry-protected corner/hinge states, we provide a physical picture based on dimensional reduction analysis and a classification and construction based on the Künneth formula of group cohomology. These strong HOSPT phases support topological boundary excitations robust against general perturbations such as disorders and crystalline distortions, and should be differentiated from weak crystalline SPT phases whose surface states are protected by crystalline symmetries. Focusing on the case where the total symmetry $G = G_c \times G_0$ is a direct product of crystalline symmetry G_c and onsite symmetry G_0, we show that a $(k+1)$th-order SPT phase in d spatial dimensions can be built from G_0-SPT phases in $(d-k)$ dimensions, and is fully classified within group cohomology formula $\mathcal{H}^k(G_c^*, \mathcal{H}^{d+1-k}(G_0, U(1)))$. Based on a decorated domain-wall picture for this group cohomology formula, we show how to explicitly construct a HOSPT phase using lower-dimensional SPT phases as building blocks.

To conclude, we briefly discuss the limitations of the group cohomology classification (1) of HOSPT phases from Künneth formula. One implicit assumption for the above classification is that the local Hilbert space always forms a linear representation of the total symmetry group. If we consider the local Hilbert space $\mathcal{S}(\alpha)$ at a high-symmetry Wyckoff position α, such as the C_4 rotation center in Fig. 2, the local Hilbert space should also preserve the "local symmetry" $G_c(\alpha) = C_4$ in addition to the onsite symmetry G_0. In the group cohomology classification (1), we always require such a local Hilbert space $\mathcal{S}(\alpha)$ to form a linear representation of local symmetry $G_c(\alpha) \times G_0$. In particular, the local crystalline symmetry operations in $G_c(\alpha)$ must commute with all onsite symmetry in G_0. Failure of this requirement [i.e., projective representations of local symmetry $G_c(\alpha) \times G_0$] may lead to even more interesting consequences, such as Lieb-Schultz-Mattis theorems forbidding a short-ranged-entangled ground state [37], which are beyond the description of formula (1).

One natural direction to expand this work is to go beyond a direct product of onsite and crystalline symmetries, and to consider the HOSPT phases with a generic symmetry group. While the Künneth formula does not simply apply for a generic symmetry group, the dimensional reduction arguments appear to remain valid. Another interesting direction is to use the same approach to study HOSPT phases of interacting fermions. We leave these for future works.

Note added. Recently, we became aware of two independent works which studied the general classification of crystalline SPT phases (with onsite and crystalline symmetries) using spectral sequence: one by Else and Thorngren [55], and one by Qi and Fang [56]. Their works have partial overlaps with this work.

ACKNOWLEDGMENTS

We are indebted to D. Else, Y. Ran, and S. Jiang for helpful discussions, to C. Fang for feedbacks on the draft, and especially to D. Else for pointing out a mistake in the manuscript. Y.-M.L. also thanks Aspen Center for Physics for hospitality, where part of this work was performed. This work is supported by NSF under Award No. DMR-1653769 (A.R., Y.-M.L.), and in part by NSF Grant No. PHY-1607611 (Y.-M.L.).

[1] M. Z. Hasan and C. L. Kane, Rev. Mod. Phys. **82**, 3045 (2010).
[2] M. Z. Hasan and J. E. Moore, Annu. Rev. Condens. Matter Phys. **2**, 55 (2011).
[3] X.-L. Qi and S.-C. Zhang, Rev. Mod. Phys. **83**, 1057 (2011).
[4] X. Chen, Z.-C. Gu, Z.-X. Liu, and X.-G. Wen, Phys. Rev. B **87**, 155114 (2013).
[5] T. Senthil, Annu. Rev. Condens. Matter Phys. **6**, 299 (2015).
[6] J. Maciejko, T. L. Hughes, and S.-C. Zhang, Annu. Rev. Condens. Matter Phys. **2**, 31 (2011).
[7] W. A. Benalcazar, B. A. Bernevig, and T. L. Hughes, Science **357**, 61 (2017).
[8] W. A. Benalcazar, B. A. Bernevig, and T. L. Hughes, Phys. Rev. B **96**, 245115 (2017).
[9] Z. Song, Z. Fang, and C. Fang, Phys. Rev. Lett. **119**, 246402 (2017).
[10] J. Langbehn, Y. Peng, L. Trifunovic, F. von Oppen, and P. W. Brouwer, Phys. Rev. Lett. **119**, 246401 (2017).
[11] C. Fang and L. Fu, arXiv:1709.01929.
[12] E. Khalaf, H. C. Po, A. Vishwanath, and H. Watanabe, Phys. Rev. X **8**, 031070 (2018).
[13] F. Schindler, A. M. Cook, M. G. Vergniory, Z. Wang, S. S. P. Parkin, B. A. Bernevig, and T. Neupert, Sci. Adv. **4**, eaat0346 (2018).
[14] M. Ezawa, Phys. Rev. Lett. **120**, 026801 (2018).
[15] Z. Yan, F. Song, and Z. Wang, Phys. Rev. Lett. **121**, 096803 (2018).
[16] Y. Wang, M. Lin, and T. L. Hughes, Phys. Rev. B **98**, 165144 (2018).
[17] Q. Wang, C.-C. Liu, Y.-M. Lu, and F. Zhang, Phys. Rev. Lett. **121**, 186801 (2018).
[18] L. Trifunovic and P. Brouwer, Phys. Rev. X **9**, 011012 (2019).
[19] Z. Wang, B. J. Wieder, J. Li, B. Yan, and B. A. Bernevig, Phys. Rev. Lett. **123**, 186401 (2019).
[20] A. Matsugatani and H. Watanabe, Phys. Rev. B **98**, 205129 (2018).
[21] S. Franca, J. van den Brink, and I. C. Fulga, Phys. Rev. B **98**, 201114 (2018).
[22] M. Serra-Garcia, V. Peri, R. Süsstrunk, O. R. Bilal, T. Larsen, L. G. Villanueva, and S. D. Huber, Nature (London) **555**, 342 (2018).
[23] F. Schindler, Z. Wang, M. G. Vergniory, A. M. Cook, A. Murani, S. Sengupta, A. Y. Kasumov, R. Deblock, S. Jeon, I. Drozdov *et al.*, Nat. Phys. (to be published).
[24] C. W. Peterson, W. A. Benalcazar, T. L. Hughes, and G. Bahl, Nature (London) **555**, 346 (2018). .
[25] X. Zhang, H.-X. Wang, Z.-K. Lin, Y. Tian, B. Xie, M.-H. Lu, Y.-F. Chen, and J.-H. Jiang, Nat. Phys. **15**, 582 (2019).
[26] R.-J. Slager, A. Mesaros, V. Juričić, and J. Zaanen, Phys. Rev. B **90**, 241403(R) (2014).
[27] B. R. Dumitru Calugaru and V. Juricic (unpublished).
[28] Z. Song, T. Zhang, Z. Fang, and C. Fang, Nat. Commun. **9**, 3530 (2018).
[29] O. Dubinkin and T. L. Hughes, Phys. Rev. B **99**, 235132 (2019).
[30] Y. You, T. Devakul, F. J. Burnell, and T. Neupert, Phys. Rev. B **98**, 235102 (2018).
[31] S. Jiang and Y. Ran, Phys. Rev. B **95**, 125107 (2017).
[32] R. Thorngren and D. V. Else, Phys. Rev. X **8**, 011040 (2018).
[33] J. C. Y. Teo and C. L. Kane, Phys. Rev. B **82**, 115120 (2010).
[34] X.-G. Wen, Phys. Rev. B **85**, 085103 (2012).
[35] H. Song, S.-J. Huang, L. Fu, and M. Hermele, Phys. Rev. X **7**, 011020 (2017).
[36] F. Lu, B. Shi, and Y.-M. Lu, New J. Phys. **19**, 073002 (2017).
[37] S.-J. Huang, H. Song, Y.-P. Huang, and M. Hermele, Phys. Rev. B **96**, 205106 (2017).
[38] A. Vishwanath and T. Senthil, Phys. Rev. X **3**, 011016 (2013).
[39] C. Wang and T. Senthil, Phys. Rev. B **87**, 235122 (2013).

[40] A. Kapustin, arXiv:1403.1467.
[41] A. Kapustin, arXiv:1404.6659.
[42] A. Kitaev, Ann. Phys. **321**, 2 (2006).
[43] Y.-M. Lu and A. Vishwanath, Phys. Rev. B **86**, 125119 (2012).
[44] X.-G. Wen, Phys. Rev. B **89**, 035147 (2014).
[45] X.-G. Wen, Phys. Rev. B **91**, 205101 (2015).
[46] M. Cheng, M. Zaletel, M. Barkeshli, A. Vishwanath, and P. Bonderson, Phys. Rev. X **6**, 041068 (2016).
[47] L. Fu, C. L. Kane, and E. J. Mele, Phys. Rev. Lett. **98**, 106803 (2007).
[48] Y. Ran, arXiv:1006.5454.
[49] H. Song and M. Hermele, Phys. Rev. B **91**, 014405 (2015).
[50] X. Chen, Y.-M. Lu, and A. Vishwanath, Nat. Commun. **5**, 3507 (2014).
[51] A. M. Turner, F. Pollmann, and E. Berg, Phys. Rev. B **83**, 075102 (2011).
[52] L. Fidkowski and A. Kitaev, Phys. Rev. B **83**, 075103 (2011).
[53] X. Chen, Z.-C. Gu, and X.-G. Wen, Phys. Rev. B **83**, 035107 (2011).
[54] N. Schuch, D. Perez-Garcia, and I. Cirac, Phys. Rev. B **84**, 165139 (2011).
[55] D. V. Else and R. Thorngren, Phys. Rev. B **99**, 115116 (2019).
[56] Z. Song, C. Fang, and Y. Qi, arXiv:1810.11013.